Feature Extraction in an Iris based recognition system using Independent Component Analysis Algorithm

A Thesis submitted in partial fulfillment of the requirements for the award of degree of

Master of Engineering
in
Electronic Instrumentation and Control

Submitted by
PARUL SETHI
(Roll No. 801051011)

Under the Guidance
of
Dr. Sunil Kumar Singla
Assistant Professor

Department of Electrical and Instrumentation Engineering

Thapar University
(Established under the section 3 of UGC act, 1956)

Patiala, 147004, Punjab, India
July 2012

DECLARATION

I hereby certify that the work is being presented in the thesis work entitled **"Feature Extraction in an Iris based recognition system using Independent Component Analysis"** in partial fulfillment of award of degree of **Master of Engineering** in **Electronics Instrumentation and Control** submitted in Electrical and Instrumentation Engineering department, Thapar University, Patiala is an authentic record of my own work carried under the supervision of **Dr. Sunil Kumar Singla,** Assistant Professor, Department of Electrical and Instrumentation Engineering, Thapar University, Patiala, Punjab.

Parul

Date:

Parul Sethi

801051011

I certify that the above statement made by the student is correct to the best of my knowledge and belief.

21/6/2012

Date:

Dr. Sunil Kumar Singla
Assistant Professor,
Department of Electrical
and Instrumentation Engineering,
Thapar University, Patiala,
Punjab

S. Ghosh 3/7/12

Dr. Smarajit Ghosh
Head of Department,
Department of Electrical and
Instrumentation Engineering,
Thapar University, Patiala,
Punjab

Countersigned by

Dr. Saroj Kumar Mohapatra
Dean of Academic Affairs,
Thapar University, Patiala,
Punjab

Abstract

The motivation of this research work is that the iris identification systems are the most authentic biometric system since iris patterns are unparallel to each individual and do not vary with time. After the development of first commercial system given by J. Daugman a variety of methods were innovated to handle eye data in biometric systems. In recent years, considerable progress has been made in the area of iris recognition. Although, the development of the numerous technologies for iris recognition has been made and they have surpassed many iris identification systems, the problem of iris recognition under gross variation remains predominately unresolved. Eye images utilized in iris recognition systems necessitate images to be carried under inflexible constraints. In order to obtain a good quality image, user's cooperation is required like the user must look directly into camera with a proper illumination in the environment etc.

In this thesis, we have focused on the area of iris localization or segmentation and blind source separation. Iris localization is the most significant part of iris recognition which requires extraction of iris boundaries in an iris image. We have developed the frame work for the iris segmentation in which iris boundary has been detected. The framework developed here is suitable only for the CASIA iris database and do not exclude the eyelashes parts inside the iris circular boundary. On the other hand a signal processing based algorithm i.e. independent component analysis (ICA) has been tested on the image which has given significant results. ICA has better performed on iris images in order to render satisfactory measures of accuracy. This dissertation discusses an approach towards less constraint iris recognition using occluded images. The ICA is implemented for a database of 200 images along with the iris localization for making a better iris recognition system.

Acknowledgement

I express my gratitude to my supervisor and mentor Dr. Sunil Kumar Singla for his kind guidance during the entire period of the research work. His consistent support, motivational words and advices helped me to complete my research project successfully. His research experience devoted me insights into my dissertation, realizing various expressions of this research field. The time and exertion he spent with me on my research polished my thesis giving an ever-lasting influence.

I really appreciate the help and motivation received from Ph.D fellow, Mr. Punit Mishra. His knowledge and acquirements with signal processing proficiencies have given lots of help with my project build up.

Finally, I would like to thank my parents, my long-time, firm assistants and consultants, who backed me up both emotionally and financially. I am also thankful to my brother who was my colleague, who encouraged me throughout my research work. He helped me in the implementation of the algorithm and its methodology in an effective and successive manner.

Parul

Place: Thapar University, Patiala — Parul Sethi

Date: — 801051011

TABLE OF CONTENTS

LIST OF FIGURES

LIST OF TABLES

Chapter 1

Introduction

The science and technology of measuring and analyzing biological data is known as Biometrics. It refers to technologies that measure and analyze human body characteristics, such as DNA, fingerprints, eye retinas and irises, voice patterns, facial patterns and hand measurements, for authentication purposes. By authentication we mean, any process by which a system verifies the identity of a user who wishes to access it. Since access control is normally based on the identity of the user who requests access to a resource, authentication is essential to effective security. Authentication is implemented, commonly by using credentials, each of which is composed of a user ID and password. Knowledge of the password is assumed to guarantee that the user is authentic. Each user registers initially, using an assigned or self-declared password. On each subsequent use, the user must know and use the previously declared password. The weakness in this system for transactions that are significant (such as the exchange of money) is that passwords can often be stolen, accidentally revealed, or forgotten [1].

Authentication by biometric verification is becoming increasingly common in corporate and public security systems, consumer electronics and point of sale (POS) applications. Biometric verification is any means by which a person can be uniquely identified by evaluating one or more distinguishing biological traits. Unique identifiers include fingerprints, hand geometry, earlobe geometry, retina and iris patterns, voice waves, DNA, and signatures. Figure 1.1 shows the biometric identifiers.

Biometric verification has advanced considerably with the advent of computerized databases and the digitization of analog data, allowing for almost instantaneous personal identification. No matter what biometric methodology is used, the identification verification process remains the same [1]. A record of a person's unique characteristic is captured and kept in a database. Later on, when identification verification is required, a new record is captured and compared with the previous record in the database. If the data in the new record matches that in the database record, the person's identity is confirmed.

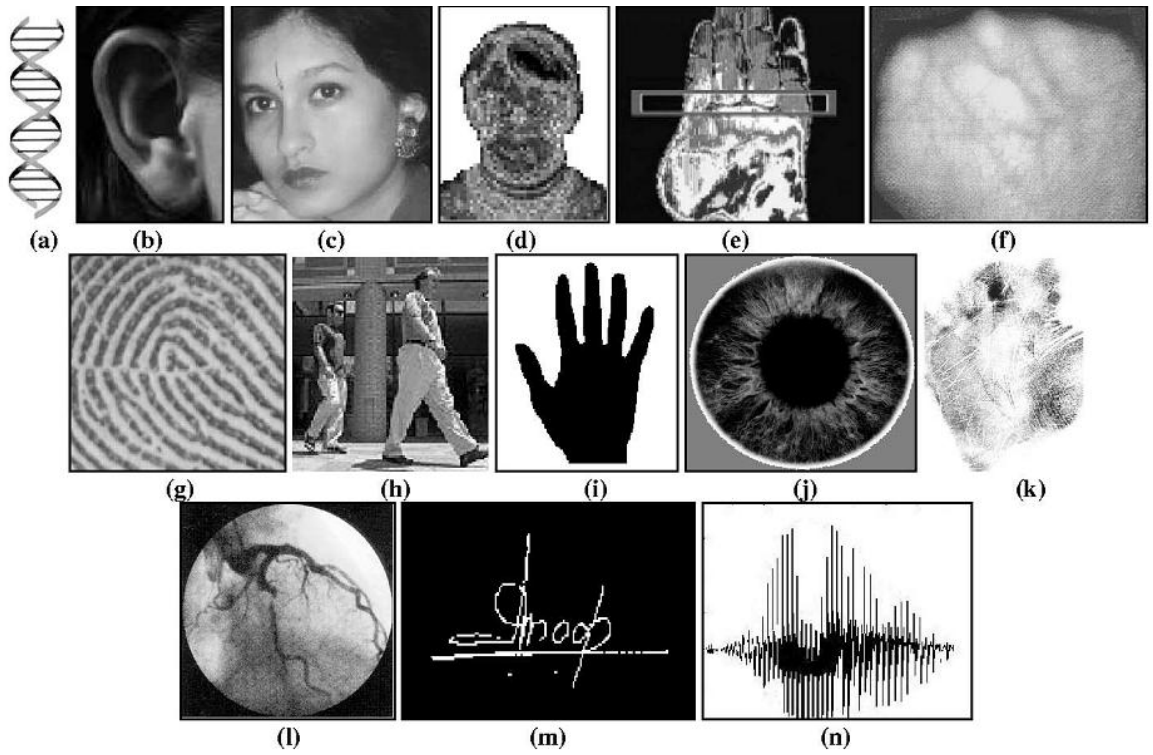

Figure 1.1 Examples of biometric characteristics: (a) DNA, (b) ear, (c) face, (d) facial thermo gram, (e) hand thermo gram, (f) hand vein, (g) fingerprint, (h) gait, (i) hand geometry, (j) iris, (k) palm print, (l) retina, (m) signature, and (n) voice[1].

Biometric authentication consists of methods for uniquely recognizing humans based upon one or more intrinsic physical or behavioral traits. Biometrics is a study and measurement of these physical characteristics and traits that are different in each one of us and to possibly use it as a differentiator when distinguishing us. Any human physiological and/or behavioral characteristic can be used as a biometric characteristic as long as it satisfies the following requirements: Universality: each person should possess the trait; Distinctiveness: any two persons should be sufficiently different in terms of the characteristic; Permanence: relates to the manner in which a trait varies over time; Collectability: the characteristic can be measured quantitatively.

However, in a practical biometric system (i.e., a system that employs biometrics for personal recognition), there are a number of other issues that should be considered, including: Performance, which relates to the accuracy, speed, and robustness of technology used; Acceptability, which indicates the extent to which people accept the use of a particular

biometric characteristic in their daily lives; Circumvention, which reflects how easily the system can be fooled using fraudulent methods [1].

1.1 Different Biometric Modalities

The most common biometric modalities include fingerprint, face, iris, voice, hand geometry, palm print etc. There is no single biometric modality that is best for all implementations. Each modality has its advantages and disadvantages. Many factors must be taken into account when implementing a biometric system including location, security risks, task (identification or verification), expected number of users etc. In this section, a brief introduction of different biometric modalities has been presented.

1.1.1Fingerprint Identification

The oldest form of biometric verification is fingerprinting. Historians have found examples of thumbprints being used as a means of unique identification on clay seals in ancient China. A fingerprint is an impression of the friction ridges of all or any part of the finger. A friction ridge is a raised portion of the on the palmer (palm) or digits (fingers and toes) or plantar (sole) skin, consisting of one or more connected ridge units of friction ridge skin. These ridges are sometimes known as "dermal ridges" or "dermal ". The traditional method uses the ink to get the finger print onto a piece of paper. This piece of paper is then scanned using a traditional scanner. Now in modern approach, live finger print readers are used. These are based on optical, thermal, silicon or ultrasonic principles [2, 3, 4]. The finger print obtained from an Optical Fingerprint Reader is shown in Figure 1.2.

Figure 1.2 Fingerprint bitmap [http://www.synel.co.uk/blog/?Tag=Biometric%20Technology]

Finger print matching techniques can be placed into two categories. One of them is minutiae based and the other one is correlation based. Minutiae based techniques find the minutiae points first and then map their relation placement on the finger. Correlation based techniques

require the precise location of a registration point and are affected by image translation and rotation [5, 6, 7, 8, 9].

Fingerprint images contain a large amount of data. Because of the high level of data present in the image, it is possible to eliminate false matches and quickly reduce the number of possible matches to a small number, even with large database sizes. Because of the fact that fingerprint imaging systems use more than one finger image in the match process, the match discrimination process is geometrically increased.

1.1.2 Facial Recognition

A facial recognition technique is an application of computer for automatically identifying or verifying a person from a digital image or a video frame from a video source. It is the most natural means of biometric identification [10]. Facial recognition technologies have recently developed into two areas and they are Facial metric and Eigen faces. Facial metric technology relies on the manufacture of the specific facial features (the system usually look for the positioning of eyes, nose and mouth and distances between these features), shown in Figure 1.3 and 1.4.

Figure 1.3: Recognition of face from body
[http://researcher.ibm.com/researcher/view_project_subpage.php?id=1926]

Figure 1.4: Normalized face [http://techplz.com/2011/05/18/recognizeme-the-first-face-recognition-security-for-jailbroken-iphone/]

The Eigen Face method (Figure 1.5) is based on categorizing faces according to the degree of it with a fixed set of 100 to 150 Eigen faces. The Eigen faces that are created will appear as light and dark areas that are arranged in a specific pattern. This pattern shows how different features of a face are singled out. It has to be evaluated and scored [9, 11, 12, 13, 14].

Figure 1.5: Eigen Face [http://www.ijofcs.org/dissertation-quintiliano.html]

Facial-recognition technology has been used by law enforcement to pick out individuals in large crowds with considerable reliability.

1.1.3 Hand Geometry

Hand geometry recognition systems are widely used for applications in physical access, attendance tracking and personal verification. They have found a sustainable market through use in security and accountability applications. Their ease of use, stand-alone capabilities, and small data requirements make them a popular choice for those in need of authentication systems.

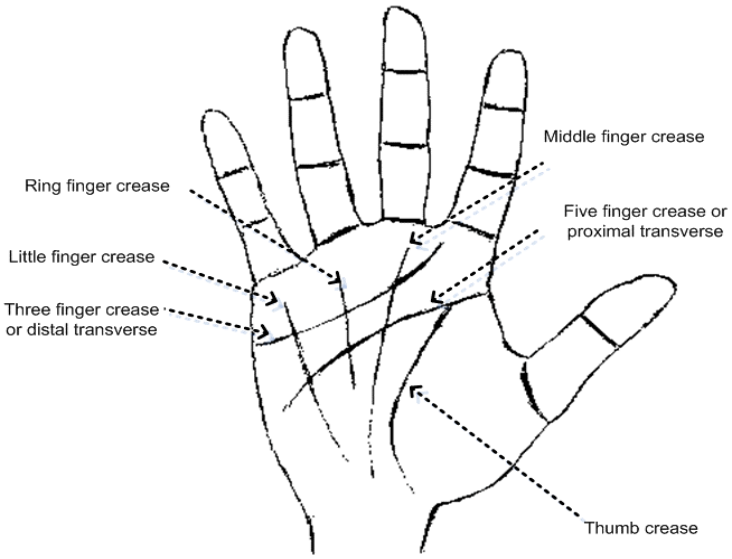

Figure 1.6: Hand geometry [http://is692sp10sm.blogspot.com/]

Hand-geometry-based systems require the subject to place his or her hand (usually the right hand) on a plate where it is photographically captured and measured. This method measures certain key features of the hand like length of fingers and thumb, the width between two points, thickness, surface area of an individual's hand etc [15]. The image captures both the top surface of the hand and a side image that is captured using an angled mirror. Hand geometry data is easier to collect. The user has to perform an obtrusive task (placing his or her hand on the platen for sampling), because of this obtrusiveness, subjects cannot have their biometric features sampled without their knowledge. So, hand-based biometric represent less of a privacy threat than some other systems also hand geometry can be easily integrated with other Biometric [15] but, it has the limited accuracy. Shape of every person's hand is not necessarily different than another person's hand also the shape of a person's hand changes significantly over a time period.

1.1.4 Retinal Scan

Retinal Scan technology is based on the blood vessel pattern in the retina of the eye. An infrared light source is used to illuminate the retina of the eye; the infrared energy is absorbed faster by blood vessels in the retina than by surrounding tissue. The image of the enhanced blood vessel pattern of the retina is analyzed for characteristic points within the pattern.

A retinal scan can produce almost the same volume of data as a fingerprint image analysis. Based on the fact that a high data volume equates to a high discrimination rate (identification rate), it would seem that retinal scan may be an alternative to fingerprint identification.

Retinal scan technology has several drawbacks that are not common to fingerprint imaging technology; 1) the retinal scan is more susceptible to disease (notably cataracts, etc.) that change the characteristics of the eye; 2) the method of obtaining a retinal scan is personally invasive - a laser light (or other coherent light source) must be directed through the cornea of the eye; and 3) the method of obtaining a correct retinal scan depends heavily on the skill of the operator and the ability of the person being scanned to follow directions.

Importantly, retinal scan technology has not had the level of research and development funding (both from private and government sources) that fingerprint imaging technology has had within the past twenty years [16].

1.1.5 Iris Scan

This recognition method uses the iris of the eye which is colored area that surrounds the pupil. Iris patterns are unique and are obtained through video based image acquisition system. Each iris structure features a complex pattern. This can be a combination of specific characteristics known as corona, crypts, filaments, freckles, pits, furrows, striations and rings [17]. An IRIS image is shown in Figure 1.7.

Figure 1.7: Image of IRIS [http://en.wikipedia.org/wiki/Iris_(anatomy)]

The iris pattern is taken by a special gray scale camera in the distance of 10-40 cm of camera. Once the gray scale image of the eye is obtained then the software tries to locate the iris within the image. When iris is found, then software creates a net of curves covering the iris.

Based on the darkness of the points along the lines the software creates the iris code. Here, two influences have to be taken into account. First, the overall darkness of image is influenced by the lighting condition so the darkness threshold used to decide whether a given point is dark or bright, it must be dynamically computed according to the overall picture darkness. Secondly, the size of the iris changes as the size of the pupil changes. Before computing the iris code, a proper transformation must be done.

In decision process, the matching software takes two iris codes and compute the hamming distance based on the number of different bits. The hamming distances score (within the range 0 means the same iris codes), which is then compared with the security threshold to make the final decision. Computing the hamming distance of two iris codes is very fast (it is the fact only counting the number of bits in the exclusive OR gate of two iris codes). We can also implement the concept of template matching in this technique. In template matching, some statistical calculation is done between a stored iris template and a captured one [9, 17, 18].

1.1.6 Vascular Patterns

Vascular pattern technology is very similar to Retinal Scan technology in that it uses infrared light to produce an image of the vein pattern in the face, in the back of a hand, or on the wrist. Vascular pattern technology is generally acceptable to users except that some users still object to any biometric method that uses infrared [16].

1.1.7 Signature Verification

The signature dynamics recognition is based on the dynamics of making the signature, rather than a direct comparison of the signature itself. The dynamics is measured as a means of the pressure, direction, acceleration and the length of the strokes, dynamics number of strokes and their duration. The most obvious and important advantage of this is that a fraudster cannot glean any information on how to write the signature by simply looking at one that has been previously written. There are various kinds of devices used to capture the signature dynamics. These are either traditional tablets or special purpose devices. Tablets capture 2D coordinates and the pressure [19, 20], Figure 1.8.

Figure 1.8: A Signature taken using Tablet [http://www.vision.caltech.edu/mariomu/research/sigverif/]

Special pens are able to capture movements in all three dimensions. Tablets have two significant disadvantages. First, the resulting digitalized signature looks different from the usual user signature. Secondly, while signing the user does not see what he or she has already written? He/she has to look at the computer monitor to see the signature [1, 9, 21]. This is a considerable drawback for many (inexperienced) users.

1.1.8 Voice Dynamics

Voice is a combination of physiological and behavioral biometric. The features of an individual's voice are based on the shape and size of the appendages (e.g., vocal tracts, mouth, nasal cavities, and lips) that are used in the synthesis of the sound [22]. These physiological characteristics of human speech are invariant for an individual, but the behavioral part of the speech of a person changes over time due to age, medical conditions such as common cold, emotional state, etc [23].

The automatic recognition process of the human voice is often divided in speech recognition and speaker recognition [15]. These two areas use the same input signal (the voice), but not for the same purpose, the speech recognition aims to recognize the message uttered by any speaker, and the speaker recognition wants to identify the person who is talking. This method captures the sound of the speaker's voice as well as the linguistic behaviors. The speaker-specific characteristics of speech are due to differences in physiological and behavioral aspects of the speech production system in humans [25]. These systems rely on very low-cost devices (hardware requirement is very low), they are generally the least expensive systems to implement for large numbers of users and the acceptability level is very high in this type of biometric system. It would allow a remote verification using the phone such as phone banking but, these systems suffers from drawbacks like mimicry by imposter or recording the voice of the authorized person or emotional statement of the authorized person [22].

1.1.9 Palm Print

Palm print, the inner surface of our palm normally contains three flexion creases, secondary creases and ridges. The flexion and secondary creases are also called principal lines and wrinkles respectively. The flexion creases and the main creases are formed between the 3rd and 5th months after conception [26] and superficial lines appear after birth. These creases are not genetically deterministic. Even identical twins who share the same DNA sequences have different palm print [27].

These non-genetically deterministic and complex patterns have rich information for personal identification. There are two types of palm print recognition research, high resolution and low resolution approaches. High resolution approach is suitable for forensic applications such as criminal detection, while low resolution is more suitable for civil and commercial applications such as access control.

Figure 1.9: Palm print (a) High resolution image (b) Low resolution image
[http://blog.cleveland.com/metro/2010/10/palm_prints_being_added_to_ohi.html]

The advantage of using palm print is that they cannot be acquired without the knowledge of the person. Moreover, the uniqueness and permanence of palm print is also high while its universality is medium.

1.1.10 DNA Technique

DNA sampling is rather intrusive at present and requires a form of tissue, blood or other bodily sample. This method of capture still has to be refined. So far the DNA analysis has not been sufficiently automatic to rank the DNA analysis as a biometric technology. The analysis of human DNA is now possible within 10 minutes. As soon as the technology advances so that DNA can be matched automatically in real time, it may become more significant. At

present Biometric Systems DNA is very entrenched in crime detection and so will remain in the law enforcement area for the time being [1, 5, 9].

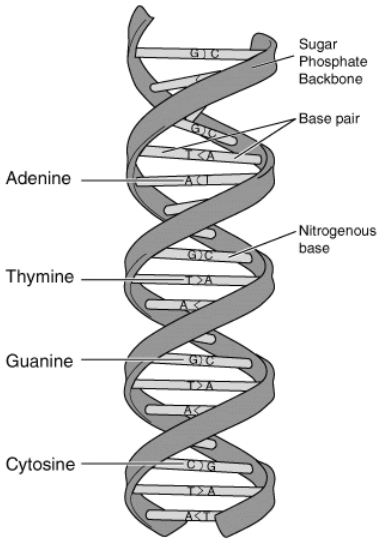

Figure 1.10: DNA biometric [http://www.dna-sequencing-service.com/dna-sequencing/dna-hydrogen-bonds/]

1.1.11 Keystroke Dynamics

Keystroke dynamics is a method of verifying the identity of an individual by their typing rhythm which can cope with trained typists as well as the amateur two-finger typist. Systems can verify the user at the log-on stage or they can continually monitor the Biometric Systems 32 typist. These systems should be cheap to install as all that is needed is a software package [9, 28, 29].

1.1.12 Hand Vein

Hand vein geometry is based on the fact that the vein pattern is distinctive for various individuals. The veins under the skin absorb infrared light and thus have a darker pattern on the image of the hand taken by an infrared camera. The hand vein geometry is still in the stage of research and development. One such system is manufactured by British Technology Group. The device is called Vein check and uses a template with the size of 50 bytes [1, 9, 30].

1.2 Factors of Evaluation

There are various parameters with the help of which one can measure the performance of any biometric authentication techniques. These factors are described below [9, 31, 32, 33].

1.2.1 False Accept Rate (FAR) or False Match Rate (FMR): The probability that the system incorrectly declares a successful match between the input pattern and a non matching pattern in the database. It measures the percent of invalid matches. These systems are critical since they are commonly used to forbid certain actions by disallowed people.

1.2.2 False Reject Rate (FRR) or False Non-Match Rate (FNMR): The probability that the system incorrectly declares failure of match between the input pattern and the matching template in the database. It measures the percent of valid inputs being rejected.

1.2.3 Relative Operating Characteristic (ROC): In general, the matching algorithm performs a decision using some parameters (e.g. a threshold). In biometric systems the FAR and FRR can typically be traded off against each other by changing those parameters. The ROC plot is obtained by graphing the values of FAR and FRR, changing the variables implicitly. A common variation is the Detection Error Tradeoff (DET), which is obtained using normal deviate scales on both axes. This more linear graph illuminates the differences for higher performances (rarer errors)

1.2.4 Equal Error Rate (EER): The rates at which both accept and reject errors are equal. ROC or DET plotting is used because how FAR and FRR can be changed, is shown clearly. When quick comparison of two systems is required, the ERR is commonly used. Obtained from the ROC plot by taking the point where FAR and FRR have the same value. The lower the EER, the more accurate the system is considered to be.

1.2.5 Failure to Enroll Rate (FTE or FER): The percentage of data input is considered invalid and fails to input into the system. Failure to enroll happens when the data obtained by the sensor are considered invalid or of poor quality.

1.2.6 Failure to Capture Rate (FTC): Within automatic systems, the probability that the system fails to detect a biometric characteristic when presented correctly is generally treated as FTC.

1.3 Biometric Authentication Systems

Biometric devices consist of a reader or scanning device, software that converts the gathered information into digital form, and a database that stores the biometric data for comparison with previous records. When converting the biometric input, the software identifies specific points of data as match points. The match points are processed using an algorithm into a value that can be compared with biometric data in the database. All biometric authentications require comparing a registered or enrolled biometric sample (biometric template or identifier) against a newly captured biometric sample (for example, a fingerprint captured during a login).

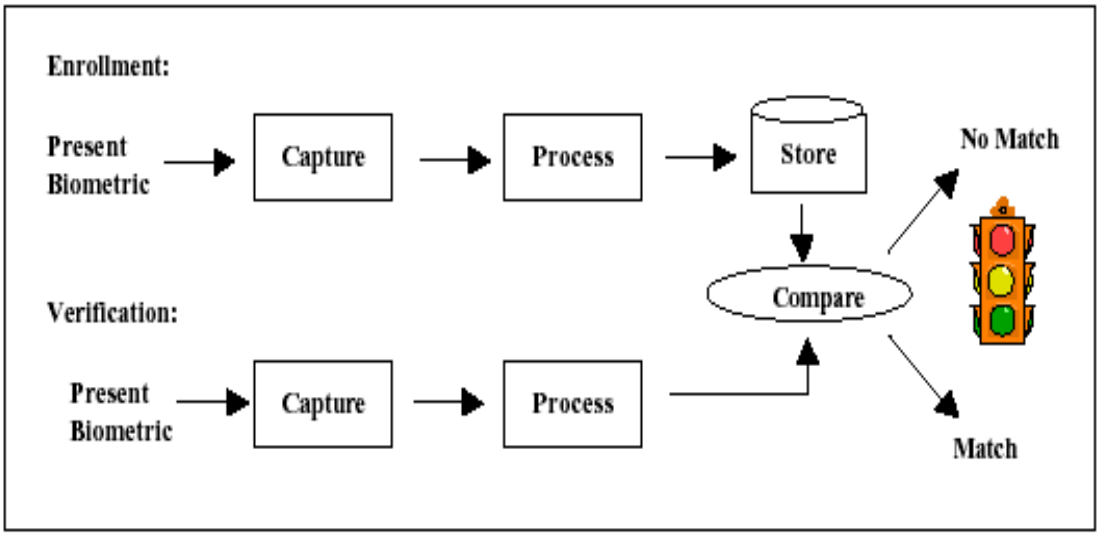

Figure 1.11: Enrollment and Verification Technique[http://www.emeraldinsight.com/mobile/index.htm?issn=0968]

1.3.1 Enrolment Mode

A sample of the biometric trait is captured, processed by a computer, and stored for later comparison. Biometric recognition can be used in Identification mode, where the biometric system identifies a person from the entire enrolled population by searching a database for a match based solely on the biometric. For example, an entire database can be searched to verify a person has not applied for entitlement benefits under two different names. This is sometimes called “one-to-many” matching.

1.3.2 Verification Mode

In this mode biometric system authenticates a person's claimed identity from their previously enrolled pattern. This is also called "one-to-one" matching. In most computer access or network access environments, verification mode would be used. A user enters an account, user name, or inserts a token such as a smart card, but instead of entering a password, a simple glance at a camera is enough to authenticate the user.

1.4 Problem Description

Iris is the concentric area located in the eye between the cornea and the lens which gives eye its color. Many researchers have worked in the area of iris recognition but there are still many areas which are required to be worked upon. The objectives of this thesis are:

1. To study the various modules of iris based recognition system
2. To collect the database
3. To preprocess the database
4. To extract the features using ICA
5. To develop the matching algorithm and find out the recognition rate.

1.5 Thesis Contribution

A review of major challenges in the various modules of iris based recognition system has been explored in detail in chapter 2. Our main aim is to extract the features or independent components in an iris. In this thesis, we deal with two important parts:

- In the first part, iris localization and segmentation is taken into consideration. Since iris is a region between the sclera and pupil, so it is important to extract only the iris area. Thus locating the iris boundary is an important pre processing method which comes under localization. There is a major problem that iris extracted is not a perfect circle, so segmentation method is required to complete it.
- In the second part, the Independent Component Analysis (ICA) technique has been applied for the iris feature extraction. Once the features have been extracted, matching of the different images of same user has been done, and matching percentage has been obtained to calculate the authenticity of the person.

Chapter 2

Literature Review

The process involved in the identification and verification of people using iris scanning and its various modules are examined in this chapter. The advantages and disadvantages associated with the utilization of iris based recognition system have been also explored. Biometric methods based on the pattern of the iris are believed to allow very high accuracy, and there has been an explosion of interest in iris biometrics in recent years.

2.1 Iris Anatomy and Performance of Biometric Systems

Iris is the concentric area located in the eye between the cornea and the lens which gives the eye its color. It is made up of tiny muscles which dilate and contract the pupil to vary the lighting conditions [34]. The process known as chaotic morphogenesis starts in the third month of gestation which causes the iris to develop in a random manner [35]. The main function of the iris is to vary the size of pupil under different lightning conditions. Two muscles, the dilator and the sphincter muscles, control the size of the iris to adjust the amount of light entering the pupil.

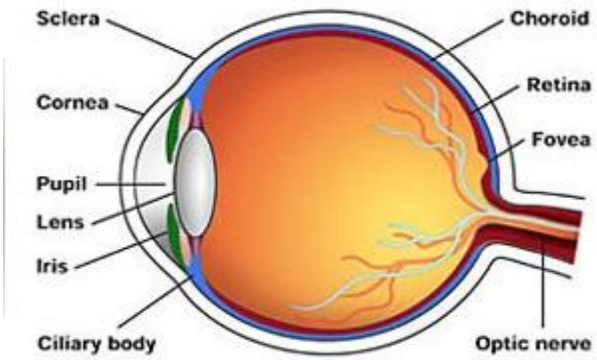

Figure 2.1: Eye anatomy http://www.visionaware.org/aging-eye-low-vision

Figure 2.1 shows an example image acquired by a commercial iris biometrics system. The iris is surrounded by sclera, a white region of connective tissue and blood vessels. Cornea is the one which covers the iris and the pupil. The pupil region generally appears darker than the iris. The iris typically has a rich pattern of furrows, ridges, pigment spots etc. The surface

of the iris is composed of two regions, the central pupillary zone and the outer ciliary zone. The collarette is the border between these two regions [36].

2.2 History of Iris Biometric System

The "early history" of iris biometrics can be considered as approximately up through 2001. Iris biometric research accelerated and broadened dramatically since 2001. For example, about forty of the iris biometric publications were published in 2006. Many iris biometrics publications, including patents are mentioned in this survey.

2.2.1 Flom and Safir's Concept Patent

The idea of using the iris as a biometric is over 100 years old [37]. However, automating then iris recognition is much more recent. In 1987, a patent was obtained by Flom and Safir for an unimplemented conceptual design of an automated iris based biometric recognition system [38]. Their patent included many conditions such as a headrest, a target image to direct the subject's gaze, and a manual operator. To check for the dilation and contraction, they suggested changing the illumination to force the pupil to a predetermined size. The description which they gave, were earlier found to be impractical as far as the imaging conditions were considered, but later they influenced in many researches. They suggested the use of pattern recognition tools, including difference operators, edge detection algorithms, and the Hough transform, to extract iris descriptors.

A report was published by Johnston [39] in 1992, where an analysis was made to check the feasibility of iris recognition which was conducted at Los Alamos National Laboratory. Around 650 iris images were acquired which were under analysis for over a 15-month period. It was found that the pattern of an individual iris remained unchanged over that period.

2.2.2 Daugman's approach

Most of the contribution in the area of iris recognition in early era was made by John Daugman. Daugman issued a patent in 1994 [40] and his early publications (e.g., [41]) included details of the operational iris recognition system. After the development of concepts of Daugman's approach, it became a standard reference model. Nearly all the existing commercial iris biometric technology is based on Daugman's work. Daugman's patent states

that “A digitized image of an eye of an individual to be identified through the video camera can be acquired by the system”. In 2004, Daugman [35] suggested to use the near-infrared illumination for image acquisition which was unintrusive to humans. Near-infrared illumination helps to give a detailed structure of heavily pigmented (dark) irises.

The systems which were structured based on Daugman’s concepts, required to position the user’s eye within the camera’s field of view. With the help of power in middle and upper frequency bands of the 2-D Fourier Spectrum, the system measures the focus of the image in real time. With the adjustment of the focus of the system, the spectral power is maximized [35]. After the image acquisition, the next step is to separate the image containing iris. The early researches in the iris segmentation presumed that the iris contained a circular boundary. However, later it was found that the pupillary and limbic boundaries were not perfectly circular. Daugman has recently analysed some alternative segmentation techniques to better model the iris boundaries [42]. After separating the iris region, the next step is to extract the features out of the iris. The first hindrance which comes in these techniques is that not all images of an iris are the same size. The size of the iris in the image is affected by the distance from the camera and the changes in illumination can cause the iris to dilate or contract. This problem was sorted mapping the extracted iris into a normalized coordinate system. Using normalization, it is assumed that the iris stretches linearly when the pupil dilates and contracts. Wyatt [43] supported this assumption but on the same side commented that it did not perfectly match the actual deformation of an iris.

When the two different images having some pixel intensities are directly compared, they will be prone to error because of differences in their lighting. Thus, for extracting the texture from the normalized iris image obtained after above steps, Daugman used the convolution with 2-dimensional Gabor filter. In this system, the filter is multiplied by the input image pixel data. After multiplication, it is then integrated over their domain of support to generate coefficients which describe, extract, and encode image information [40]. The next step after the texture extraction, is matching the input image with the store database. The iris recognition is on a very large scale, so the comparison between the two images needs to be very fast. Thus, Daugman used a technique in the texture representation, where he quantized each filter’s phase response into a pair of bits. A metric called the normalized Hamming distance was

adopted by Daugman. The Hamming distance is the number of bits that disagree, whereas the normalized Hamming distance is the fraction of bits that disagree. A low normalized Hamming distance entails strong similarity of the iris codes. This representation has several advantages such as high speed of matching through the normalized Hamming distance, easy handling of rotation of the iris and an interpretation of the matching as the result of a statistical test of independence [41]. The term, "iris code" was used by Daugman in his 1993 paper.

2.2.3 Wildes Approach

Wildes [44] uses the approach which are very much different from Daugman's approach. He developed an iris biometrics system at Sarnoff Labs. Where the image acquisition in Daugman's system was done using an LED based light source in junction with a video camera, the Wildes system used a diffused source and polarization in junction with a low light level camera. To localize the iris boundary, Daugman used the maxima in an integro-differential operator technique whereas Wildes' approach included the computation of a binary edge map followed by Hough transform to detect circles. As mentioned in the Daugman' approach, to match two irises, Daugman computed the normalized hamming distance between iris codes while on the other hand, Wildes applied a Laplacian of Gaussian at multiple scales to produce a template and computes the normalized correlation as a similarity measure.

Wildes registered two patents in 1996 and 1998, [45], in which he discussed the automated segmentation method, the normalized spatial correlation for matching, and an acquisition system allowing a user to self-position his/her eye. The paper by Wildes [46] had large number of problems which were treated recently in his book chapter [47].

2.3 Hindrances in different modules of iris recognition

The iris being a protected internal organ, whose random texture is most reliable and stable throughout life, can serve as a kind of living password that one need not to remember but always carries along. Nanavati et al. in 2002 [48] gave a concept that every iris is distinct, even two irises of the same individual, and the irises of twins are different. Iris patterns are formed before birth and do not change over the course of a lifetime. Rhodes, in 2002 [49] suggested that even medical procedures such as refractive surgery, cataract surgery, and

cornea transplants do not affect recognizable characteristics. Because of the natural protection of the eyes in the face, and the protection of the iris beneath the cornea, the iris is also resistant to injury, making it highly stable as a recognizable characteristic.

The iris recognition is basically divided into following steps. Those include i) Acquiring an image of an eye of the human to be identified, ii) isolating and defining the iris of the eye within the image, which includes defining a circular pupillary boundary between the iris and pupil portions of the image; and defining another circular boundary between the iris and sclera portions of the image, iii) analyzing the iris to generate a presenting iris code, iv) comparing said presenting code with a previously generated reference iris code to find the measure of similarity, and v) calculating a confidence level for the decision. These various steps of iris recognition are shown in Figure 2.2.

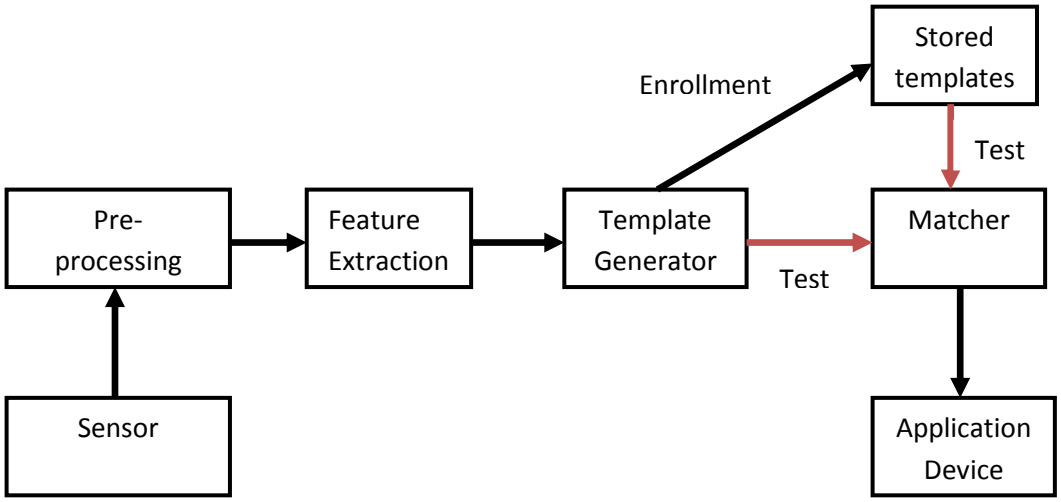

Figure 2.2 Various steps of a biometric recognition system.

2.3.1 Sensor module

Sensor is the first step in any system. The success of the iris based recognition system highly depends upon the quality of the image captured by the sensor. If in an iris recognition system the image captured is of low quality and contain random specular reflections in and around the iris, then the performance of the iris recognition based biometric system is influenced by a great amount [50].

In 1996, Sensar Inc. and the David Sarnoff Research Center by Hanna et al. [51] developed a system that would actively find the eye of the nearest user who stood between 1 and 3 feet

from cameras. Their system used two wide field-of-view cameras and a cross-correlation-based stereo algorithm to search for the coarse location of the head. They used a template-based method to search for the characteristic arrangements of features in the face. Then, a narrow field-of-view (NFOV) camera would confirm the presence of the eye and acquires the eye image. Two incandescent lights, one on each side of the camera, illuminated the face. The NFOV camera eye-finding algorithm searched for the specular reflections of these lights to locate the eye. Park et al. [52], in 2005, proposed an approach to fast acquisition of in-focus iris images, but they exploit the specular reflections that can be expected to be found in the pupil region in iris images.

Several researchers have investigated how the working volume of an iris acquisition system can be expanded. Fancourt et al. [53] in 2005 demonstrated that it is possible to acquire images at a distance of up to ten meters that are of sufficient quality to support iris biometrics. However, their system required very constrained conditions. A theoretical framework developed by He et al. [54] in 2006, discussed the acquisition of in-focus images. They have discussed the differences between fixed-focus imaging devices and auto-focus imaging devices, where the effects of illumination by different near infrared wavelengths are illustrated. They conclude that "illumination outside 700-900 nm cannot reveal the iris' rich texture".

Identity recognition is also impacted significantly when scanning images are not perfect due to lighting, motion, blur, or even physical problems like occluded irises, and others [55]. There are three main problems of concern, i.e. defocus, motion blur, and occlusion. A system that employs fixed-focus optical lens easily causes defocused iris images. Iris scanners work only when targets are stationary and within very close range, since it is impossible to capture iris images from moving targets. In 2003, Ma et al. [56] discusses that motion blurred images are captured by a CCD sensor in interlaced scan mode, and a frame is combined by two fields with an interval of 20ms or less, and the resulting image involves obvious interlacing lines in the horizontal direction. Wei et al. [57] in 2006 in his paper explained that an occluded image is the case that most area of the iris is covered by eyelid and eyelashes. It often happens if the client blinks while the images are being taken. Bachoo et al. [58] in 2005, approach the detection of eyelash occlusion using the gray-level co-occurrence matrix

(GLCM) pattern analysis technique. Possible challenges for this approach are choosing the correct window size and dealing with windows that have a mixture of types. Figure 2.3 shows the above three problems.

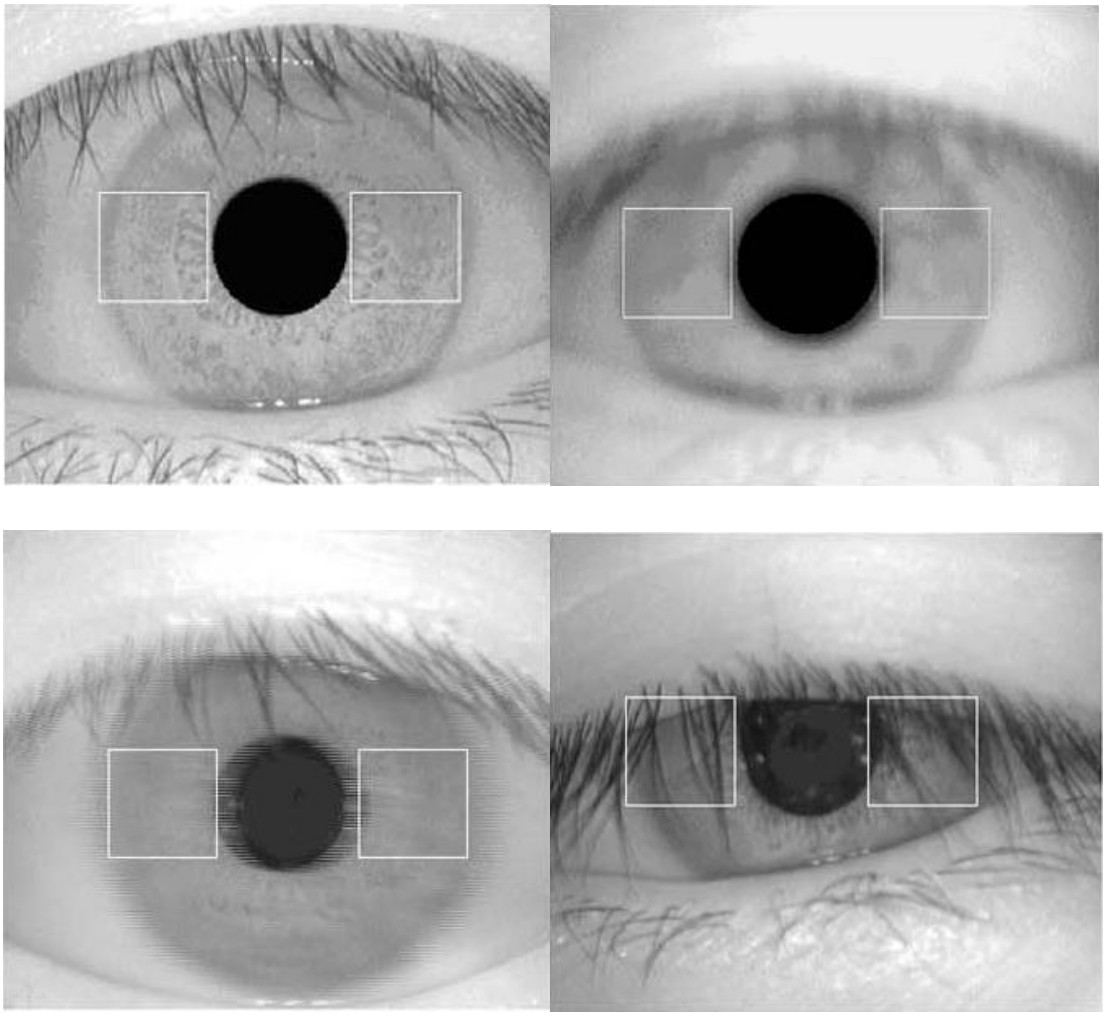

Figure 2.3 Image qualities with (a) clear image, (b) defocused image, (c) motion blurred image, and (d) occluded image [w] (Ma et al., 2003).

Most iris recognition devices are capable of capturing only one image of an iris at a time. After each image capture, the device user must manually enter several pieces of identifying information, including whether the image is of a left eye or a right eye. Hence, the single capture ability of iris recognition devices slows the data collection process and increases the likelihood that iris images will be misidentified and mislabeled [50].

Discussing more of the problems related to iris recognition includes that the optical systems may introduce image rotation depending on eye position, camera position or subject position. This is a problem for some algorithms. Daugman in his papers published in 1993 [60] and 2003 [61] computes the iris code in a single canonical orientation and compares it with several orientations by scrolling, but other iris algorithms are invariant to rotation as suggested by Avila et al., in 2005 [62]. Due to optical issues, subject motion, illumination limitation, good quality iris image acquisition becomes very difficult and these difficulties are mentioned in papers published by Jain et al., in 2004 [63]; Matey et al., in 2006 [64]; and Daugman, in 2007 [65]. Even when a good quality camera is used, the result is commonly useless for iris recognition. Auto-focus, if it is applied, usually concentrates on the face not on the iris itself, but when auto-focus is disabled then the distance between the head and the camera must to keep stable, fixed manually by the camera operator or by the user himself. Lorenz et al., in 2008 [66] gave the suggestion that this kind of acquisition reduces image quality, and is very uncomfortable to the user.

2.3.2 Preprocessing module

Iris image preprocessing is one of the most important steps in iris recognition system and affects the accuracy of matching. It includes iris localization and iris image quality evaluation. Pan et al., in 2005 [67] gave the definition of iris localization which refers to detection of the inner and outer boundaries of the iris. The localization algorithm aims for fast and accurate determination of the iris boundaries. However, in practice, accurate algorithms require a long time to locate iris which was explained by Chowhan et al., in 2009 [68]. The first step in iris localization is to detect the pupil, which is the black circular part surrounded by iris tissues. As pupil is the largest black area in the intensity image, its edges can be detected easily from the binarized image by using suitable threshold on the intensity image. But the problem of binarization arises in case of persons having dark iris and the localization of pupil fails in such cases which was explained by Gupta et al., in 2006 [69]. To convert the original image to the binary image, we need to choose a reasonable threshold value. Firstly we have to analyze the histogram of the original iris image. Figure 2.4, which is the gray level histogram of Figure 2.5, have three peaks. The image intensity values in the vicinity of the first peak represent the pupil region's intensity values. Similarly, the image intensity values near the second and the third peaks represent the intensity values of the iris

region and the sclera region, respectively. We choose the intensity value of the dip between the first and second peaks as the threshold value. Then, we convert the original iris image to the binary image. We find, in the binary image, there are some bright spots in the pupil, which gets generated under illumination. These bright spots will reduce the accuracy of localization, which were explicated by Pan et al., in 2005 [67].

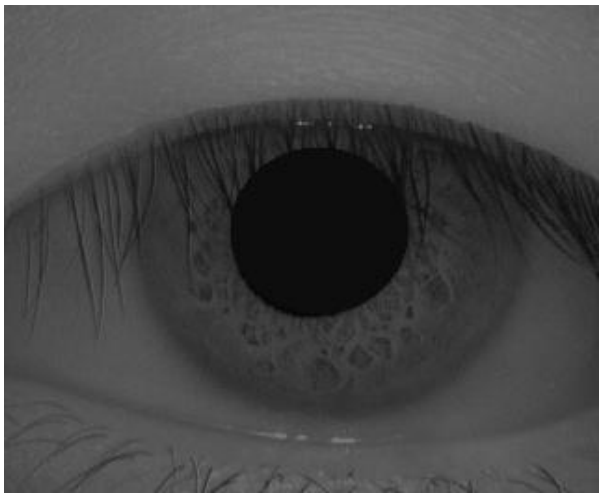

Figure 2.4 An original iris image (size 320 × 280)

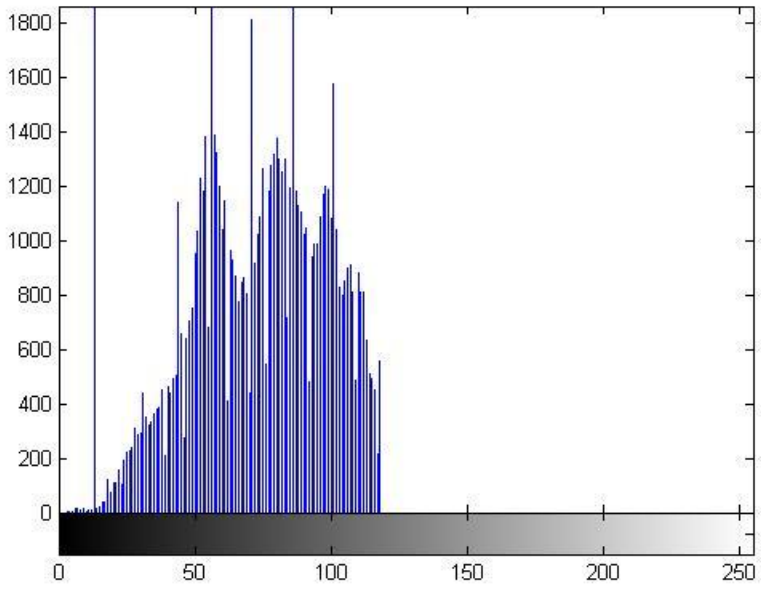

Figure 2.5 Gray level histogram of the original iris image, the intensity value of the dip between the first and the second peaks is chosen to be the threshold value.

Gonzaga et al. in 2009 [70] discussed another important consideration is that the pupil, in most of the cases, is not a perfect circumference. Since it is a muscle-filled organ (trabeculae), the contraction and dilation movements distort more and more of its pseudo-circumference. Collectively, the preprocessing of images is a lengthy stage and therefore difficult to perform manually. There is an alternative to the manual method. The automatic procedure always uses the same naming sequences at different stages of processing. In case one disastrous problem may occur here then that will permanently affect the sequences of the input images [71].

The second part in the preprocessing of iris image is iris image quality evaluation. Lei et al., in 2003 [72] discussed that the quality of some iris images is so terrible that error matching will be caused. Image quality assessment plays an important role in automated biometric systems for two reasons, (1) system performance (recognition and segmentation), and (2) interoperability. Low quality images have poor lighting defocus blur, off-angle, and heavy occlusion, which have a negative impact on even the best available segmentation algorithms which was discussed by Kalka et al., in 2006 [73].

Preprocessing also includes the processes of iris normalization, iris image enhancement and denoising. Irises of different people may be captured in different size; also, the size of the iris of the same person may change because of the variation of the illumination. Such elastic deformations in iris texture affect the results of iris matching. For the purpose of achieving more accurate recognition results, it is necessary to compensate for these deformations through normalization and these were discussed in a paper by Ma et al., in 2002 [74]. Normalization involves the process of organizing data to minimize redundancy and then dividing a database into two or more tables and defining relationships between the tables. The problems related to normalization are that the image has low contrast and may have non-uniform illumination caused by the position of light sources. So we use the concept of image enhancement by means of histogram equalization and removal of noise by filtering the image with a low pass Gaussian filter. The problem with histogram equalization is that it can produce undesirable effects when applied to images with low color depth (bits per pixel). For example, if applied to an 8-bit image displayed with 8-bit gray scale it will further reduce color depth (number of unique shades of gray) of the image. Histogram equalization will

work the best when applied to images with much higher color depth than palette size, like continuous data or 16-bit gray-scale images which has been explained by Moorthi et al., in 2010 [75].

Proenca et al. in 2006 [76] evaluated four different clustering algorithms for preprocessing the images to enhance the image contrast. The fuzzy k-means clustering algorithm used on the position and intensity feature vector was found the best. They compared their segmentation algorithms with algorithms of Daugman (1993) [60], Tuceryan (1994) [76], Wildes (1997) [77], and Camus et al. (2002) [78]. They tested these methods on the UBIRIS dataset, which contained one session of high-quality images, and other of lower-quality images. Wildes' original methodology correctly segmented the images 98.68% of the time on the good quality dataset, and 96.68% of the time on their poorer quality dataset. The algorithm by Proenca et al. (2006) [76] performed second-best with 98.02% accuracy on the good dataset, but they had the smallest performance degradation with 97.88% accuracy on the poorer quality dataset.

Denoising is done using either the mean filter or median filter. The main problem with the mean filter is that a single pixel with a very unrepresentative value affects the mean value of all the pixels in its neighborhood. When the filter neighborhood straddles an edge, the filter will interpolate new values for pixels on the edge and so will blur that edge. This is the biggest problem when a sharp edged image is required in the output. This problem is removed by the median filter. The median filter is often a better filter for reducing noise than the mean filter, but it takes longer to compute.

2.3.3 Feature extraction

The next module is related to feature extraction. High dimensional problems are becoming increasingly common. Noh et al., in 2005 [79] explained that with high dimensional data, it is difficult to understand the underlying structure. Additionally, the storage, transmission and processing of high dimensional data places great demands on systems. All these are aspects of the computational and data analysis problems discussed by Chowhan et al., in 2009 [68]. Noh et al., in 2005 [79] explained that iris feature extraction is the crucial stage of the whole iris recognition process for personal identification. A major approach for iris recognition is to generate feature vectors corresponding to individual iris images and to perform iris matching

based on some distance metrics discussed in papers by Daugman et al., in 1993 [60] and Ma et al., in 2004 [81]. Miyazawa et al., in 2005 [82] explained one of the problems in feature-based iris recognition that the matching performance is significantly influenced by many parameters in feature extraction process, which may vary depending on environmental factors of image acquisition. The human eye is sensitive to visible light. The pupil contracts and dilates under the effect of the visible light, and the iris and the sclera exceptionally reflect within this range. In order to capture an image of the human iris by using visible light, a problem occurs, how to keep the natural reflexes on the globe of the eye, iris and sclera surfaces from affecting the quality of the digital image? The NIR illumination generates good resolution and definition images. But, due to the fact that they are not "visible" to the human eye, they do not allow for the necessary stimuli so that the pupil can perform the contraction and the dilation movements. The image quality is compromised, thus making the extraction of features difficult which were explained in detail by Gonzaga et al., in 2009 [70]. These images do not provide enough quality for a dependable biometric recognition.

2.3.4 Template matching

In this module the template is compared with the other templates stored in a database until either a matching template is found and the person is identified, or no match is found and the person remains unidentified. The matching process can be done by the use of an image pyramid. This is a series of images, at different scales, which are formed by repeatedly filtering and sub-sampling the original image in order to generate a sequence of reduced resolution images as discussed by Adelson et al., in 1984 [83]. More than one template having different scales and rotations are to be used, since using a single template decreases the accuracy. Cole et al., in 2004 [84] supported the concept and explained that this improves the execution speed for comparing, images; however, the computation time still scales linearly with the size of the set. There are two error rates that need to be taken into consideration. False reject rate (FRR) occurs when the biometric measurement taken from the live subject fails to match the template stored in the biometric system. False accept rate (FAR) occurs when the measurement taken from the live subject is so close to another subject’s template that a correct match will be declared by mistake and these concepts were explicated by Khaw, in 2002 [85]. Inadequate training of users at the initial enrollment period will cause problems both at the initial enrollment time and subsequent authentications.

2.4 Feature Extraction and Selection Methods

The task of the feature extraction and selection methods is to obtain the most relevant information from the original data and represent that information in a lower dimensionality space.

2.4.1 Selection Methods

- The selection of features is needed when the cost of the acquisition and manipulation of all the measurements is high.
- The goal is to select, among all the available features, those that will perform better.
- We have to choose P variables in a set of M variables so that the separability is maximal.

2.4.2 Extraction Methods

- The goal is to transform the origin space X in a new space Y to obtain new features that work better. This way, we can compress the information.

Few of the extraction methods are discussed below:

2.4.2.1 Wavelet Encoding

Wavelets disintegrate the data in the iris region into uncorrelated components. They overcome the problems of traditional Fourier transform in which the frequency data is localized and so the features occur at the same position to be matched up. A bank of wavelets (number of wavelet filters) is applied to the two- dimensional iris region, one for each resolution with each wavelet a scaled version of some basis function. The result of applying the wavelets is further encoded to obtain a compressed and independent representation of the iris texture.

2.4.2.2 Gabor Filtering

Gabor filters are able to provide optimum conjoint representation of a signal in space and spatial frequency. A Gabor filter is constructed by modulating a sine/cosine wave with a Gaussian. This is able to provide the optimum conjoint localization in both space and frequency, since a sine wave is perfectly localized in frequency, but not localized in space. Modulation of the sine with a Gaussian provides localization in space, though with loss of localization in frequency. Decomposition of a signal is accomplished using a quadrature pair of Gabor filters, with a real part specified by a cosine modulated by a Gaussian, and an imaginary part specified by a sine modulated by a Gaussian. The real and imaginary filters

are also known as the even symmetric and odd symmetric components respectively.

2.4.2.3 Principal Component Analysis

The objective of this division is to provide a verbal description of the central ideas behind principal component analysis (PCA) tool which was developed by Karl Pearson in 1901[86]. There is a significant abstract on the expansion of distinguishable information in multivariate technologies. Karl Pearsonin developed bases for the expansion of ordinal data and the bases of the principal component analysis. Principle component analysis is an algorithm which is used for decomposition of discrete data in its simplest form. In general it is believed that, when it comes to figure out the problems of pattern classification PCA outperform other algorithms because it works for low and high dimensionality data reduction and also helps in optimizing the image reconstruction. This contributes to the useful ability in field such as face verification and image feature reduction, and is a common methodology for ascertaining various patterns of high dimensionality data.

Principal component analysis resolves the difficulties of determining the directions of the extent variation of the additive amalgamation of random vector of 2D variance-covariance. The main actuation toward the rear of this problem is that the directions of extent variance contribute maximum amount of data about the composition of the information in 2D space. In the process of data decomposition the very first principal component will have the extent variance and take out the maximum quantity of usable features from the data. Furthermore, next consecutive principal component will be extraneous to the first principal component, and will have the greater variance than the previous one, and ultimately take out maximum amount of information from data in subspace. These components subsequently made a line of projection on which consist of minimum residuals of sum of squared deviations [87].

2.4.2.2 Linear Discriminant Analysis

Linear Discriminant Analysis is also known as Fisher analysis since it was introduced by Fisher. LDA is a linear transformation. Linear Discriminant analysis (LDA) method is used in statistics, pattern recognition and machine learning to find a linear combination of features which characterizes or separates two or more classes of objects or events. The resulting combination may be used as a linear classifier or, more commonly, for dimensionality reduction before later classification [88].

In PCA, the subspace defined by the vectors is the one that better describes the conjunct of data. LDA tries to discriminate between the different classes of data.

2.4.2.3 Independent Component Analysis

The Independent Component Analysis (ICA) algorithm has recently egressed as a potent solution to blind source separation. This algorithm is a multichannel image processing method which transmutes an observed multi dimensional vector that are unknown linear mixtures of unknown independent source signals into components which are statistically independent, i.e. uncorrelated. Thus, the goal of ICA is to recover independent sources given only sensor observations that are unknown linear mixtures of the unobserved independent source signals.

The possible use of Independent Component Analysis algorithm for face recognition has been shown by Bartlett and Sejnowski [89]. Independent component analysis (ICA) method approaches to determine a linear transformation for non-Gaussian data, making the components to be statistically independent. Thus, ICA is an effective technique to separate independent sources linearly mixed in several sensors.

Assume that we observe n linear mixtures x_1, ...,x_n of n independent components

$$x_j = a_{j1}s_1+a_{j2}s_2+...+a_{jn}s_n, \text{ for all } j$$

Here, x denotes the random vector whose elements are the mixtures x_1, ...,x_n, and s denotes the random vector (sources) with elements s_1, ..., s_n. The matrix A is the mixing matrix with elements $a_{ij.}$ Using this vector-matrix notation, the above mixing model is written as:

$$x = As$$

After estimating the matrix A, we can compute its inverse, say W, and obtain the independent components simply by:

$$s = Wx$$

To measure the non gaussainity to use it in ICA estimation, there are many methods such as kurtosis, negentropy, minimization of mutual information etc. For simplification, we assume that the observed signal matrix is centered (zero-mean) and has variance equal to one. These

are few preprocessing methods which need to be enforced before applying an ICA algorithm on the data.

Overall, iris recognition provides one of the most secure methods of authentication because of its unique characteristics as mentioned earlier in this section. But there are certain hurdles in this biometric method. Each of its modules suffers certain kinds of difficulties, which have been discussed in detail in this survey section along with its evolution. Substantial work (research) is required to be performed at each and every stage of iris based biometric systems in order to have very less false acceptance and rejection rates. Also, different feature extraction methods are discussed where the identifiable features such as contraction furrows, striations, pits, collagenous fibres, filaments, crypts, freckles, strips etc are extracted.

Chapter 3

Methodology

3.1 Introduction

Iris identification schemes are the most authentic biometric system since iris patterns are unparalleled to each person and do not vary with due course of time. Although a variety of methods for iris authentication has been studied in a widespread way, it is still, not an exclusively solved problem. Eye images employed in iris identification systems need images to be acquired under inflexible restraints. To receive a good quality image, user's cooperation is required like the subject must look directly into camera, still and there should be a suitable illumination. Hence, Iris localization is the most important part of iris recognition which involves the detection of iris boundaries in an image. Other aspect of the of the iris recognition consist of various preprocessing methods such as image segmentation, data decomposition, normalization etc. In this thesis we have developed an important and novel method for iris feature extraction iris and recognition with the help of independent component analysis (ICA) algorithm.

3.2 ICA Model (Generative model)

Assume that we observe n linear mixtures $x_1, ..., x_n$ of n independent components

$$x_j = a_{j1}s_1 + a_{j2}s_2 + ... + a_{jn}s_n, \text{ for all } j \qquad \dots (3.1)$$

Let us denote by x the random vector whose elements are the mixtures $x_1, ..., x_n$, and likewise by s the random vector with elements $s_1, ..., s_n$. Let us denote by A the matrix with elements a_{ij}. Using this vector-matrix notation, the above mixing model is written as:

$$x = As \qquad \dots (3.2)$$

where, x is the observed signal; A is the mixing matrix and, S is the independent source [90].

This algorithm is also termed as blind source separation (BSS). The term blind cites that no precise and clear knowledge of source signals or mixing system is available [92]. The simple

assumption made in independent component analysis approach is that it uses statistical independence of the source signals to solve the blind signal separation problems. We also assume that the independent component must have non Gaussian distributions. However, in our model we do not assume these distributions known. For simplicity, we also assume that the unknown mixing matrix is a square. Then, after estimating the matrix A, we can compute its inverse, say W, and obtain the independent component simply by:

$$s = Wx \qquad \ldots (3.3)$$

3.3 Ambiguities of ICA

In the ICA model in Eq. (3.2), there are few of the ambiguities as mentioned below [90]:

1. We cannot determine the variances (energies) of the independent components: Since both A and s is unknown, any scalar multiplier in one of the sources could always be cancelled by dividing the corresponding column of A by the same scalar. Thus, it is assumed that each component has a variance of 1. However, this still leaves an ambiguity of sign.
2. We cannot determine the order of the independent components: Also, since both A and s is unknown, their order can vary. They are often sorted by the amount of variance of the original signal that they explain. So it is not possible to determine the order of the uncorrelated components.

3.4 Principles of ICA estimation

3.4.1 "Nongaussian is independent"

Probability theory gives an important result about the central limit theorem, which explains that the distribution of a sum of independent random variables tends toward a Gaussian distribution, under few conditions. Thus, the sum of two independent components has a distribution which is almost Gaussian than any of those two original variables.

Equation 2 can be written in the form

$$s = A^{-1}x \qquad (3.4)$$

To estimate one of the components, we consider a linear combination of the x (say y)

$$y = w^T x \qquad (3.5)$$

Where, w is a vector to be determined. If w were one of the rows of the inverse of A, this linear combination would actually equal one of the independent components [90].

Thus, the Central Limit Theorem is used to estimate w so that it approximates a row of the inverse of A. For this example it is assumed that all the independent components of s are identically distributed. A change of variables is made by adjusting $z = A^T w$. Then we have $y = w^T x = w^T A s = z^T s$. Thus y is a linear combination of s_i with weights given by their corresponding z. Since the Central Limit Theorem tells us that the sum of two independent random variables is more Gaussian than the original variable, $z^T s$ is more Gaussian than any of the s_i and becomes least Gaussian when it is equal to one of the s_i. In this case only one of the elements of z would be non-zero. Thus maximizing the non-Gaussianity of $w^T x$ gives us one of the independent components [90].

3.4.2 Measures of Nongaussanity

A couple of measures of non-Gaussianity are used to solve the ICA problem including Kurtosis and Negentropy. Also other methods used are minimizing mutual information and maximum likelihood estimation (Infomax) which is not directly measures of non-Gaussianity but lead to the same end [93].

3.4.2.1 Kurtosis

According to the Central limit theorem, nongaussianity is a firm evaluation of independency. Kurtosis which is also named as fourth order cumulant was used by higher order statistics to measure non-gaussianity. The kurtosis of a zero-mean random variable y is defined by

$$\text{kurt}(y) = E\{y^4\} - 3(E\{y^2\})^2 \qquad (3.6)$$

Where $E\{y^4\}$ = fourth moment of y

$E\{y^2\}$ = second moment of y

Kurtosis is zero for Gaussian random variable since in equation 5, the $E\{y^4\}$ equals $3(E\{y^2\})^2$. If y is a non-gaussian random variable, its kurtosis is either positive or negative. Particularly when kurtosis value is positive the random variables are called supergaussian or leptokurtic and when negative called subgaussian or platykurtic. Supergaussian random variables have a spiky probability density function with heavy tails and subgaussian random

variables have a flat probability density function. Thereore, non-gaussianity is measured by the absolute value of kurtosis [93].

3.4.2.2 Negentropy

A second very important measure of nongaussianity is given by negentropy. Negentropy is based on the information-theoretic quantity of (differential) entropy. The entropy of a random variable is defined as the degree of information that the observation of the variable gives. The more random, i.e. unpredictable and unstructured the variable is the larger is its entropy. It is found that a gaussian variable has the largest entropy among all random variables of equal variance. This means that entropy could be used as a measure of nongaussianity. This also proves that the Gaussian distribution is the most random or the least structured among all distributions. The differential entropy H of a random variable v with a density of f (y) is given by

$$H(y) = -\int f(y) \log f(y)\, dy \qquad (3.7)$$

To obtain a measure of nongaussianity that is zero for a gaussian variable and always nonnegative, one often uses a slightly modified version of the definition of differential entropy, called negentropy. Negentropy J is defined as follows

$$J(y) = H(y_{gauss}) - H(y) \qquad (3.8)$$

Where y_{Gauss} is a Gaussian random variable of the same covariance matrix as y. Negentropy is always non-negative, and it is zero if and only if y has a Gaussian distribution.

The advantage of using negentropy as a measure of nongaussianity is that it is well justified by statistical theory. In fact, negentropy is in some sense the optimal estimator of nongaussianity, as far as statistical properties are concerned. The problem in using negentropy is, however, that it is computationally very difficult.

Approximations of Negentropy

The estimation of negentropy is very difficult. In practice, some approximation has to be used. These approximations were based on the maximum-entropy principle. In general we obtain the following approximation:

$$H(y) = k [E \{G (y_i)\}-E \{G (v)\}]^2 \quad (3.9)$$

Where K is some positive constants and v is a Gaussian variable of zero mean and unit variance.

The variable y is assumed to be of zero mean and unit variance, and the functions G is some nonquadratic functions. Choosing G wisely, one obtains approximations of negentropy that are much better. If G is chosen such that it does not grow too fast, one obtains more robust estimators. The following choices of G have proved very useful:

$$G_1 (v) = 1/a_1 \log\cosh_{a1} v \quad (3.10)$$

$$G_2 (v) = -1/a_2 \exp (-a_2 v^2/2) \quad (3.11)$$

$$G_3 (v) = ¼ v^4 \quad (3.12)$$

Where a1 and a2 are some suitable constants [93].

3.4.2.3 Minimization of mutual information

Another approach for ICA estimation, inspired by information theory, is minimization of mutual information.

Mutual Information:

Mutual information is a natural measure of dependency between random variables, i.e. it is a measure of the information that member of a set of random variables have on the other random variable in the set. It is always non-negative, and zero if and only if the variables are statistically independent.

Using the concept of differential entropy, we define the mutual information I between m (scalar) random variable y_i, i = 1...m as follows

$$I (y_1, y_2 \ldots y_m) = \sum_{i=1}^{m} H(yi) . H(y) \quad (3.13)$$

Mutual information can be interpreted by using the interpretation of entropy as code length. The terms H (yi) give the lengths of codes for the yi when these are coded separately, and H(y) gives the code length when y is coded as a random vector, i.e. all the components are coded in the same code. Mutual information thus shows what code length reduction is

obtained by coding the whole vector instead of the separate components. In general, better codes can be obtained by coding the whole vector. However, if the yi are independent, they give no information on each other, and one could just as well code the variables separately without increasing code length.

An important property of mutual information [107, 108] is that we have for an invertible linear transformation y =Wx:

$$I(y1,y2, ...,yn) = \sum_i H(y_i) - H(x) - \log |\det W| \qquad (3.14)$$

Now, let us consider what happens if we constrain the y_i to be uncorrelated and of unit variance. This means $E\{yy^T\} = W E\{xx^T\} W^T = I$, which implies

$$\det I = 1 = (\det W E\{xx^T\} W^T) = (\det W)(\det E\{xx^T\})(\det W^T) \qquad (3.15)$$

and this implies that detW must be constant. Moreover, for yi of unit variance, entropy and negentropy differ only by a constant, and the sign. Thus we obtain,

$$I(y_1,y_2, ...,y_n) = C - \sum_i J(y_i). \qquad (3.16)$$

where C is a constant that does not depend on W. This shows the fundamental relation between negentropy and mutual information [90].

3.5 Normalization techniques

The different normalization methods are to be discussed here, where any one of these will be used in the ICA algorithm [94].

3.5.1 Min max normalization

$$x' = \frac{x - \min(x)}{\max(x) - \min(x)} \qquad (3.17)$$

In this method, we find the minimum (min(x)) and maximum (max(x)) values of a given data and using these values in the above formula, we can calculate its normalized value.

3.5.2 Z-score normalization

Z-score normalization method calculates normalized values using arithmetic mean and standard deviation of the given data. The normalized values will have a spread with mean of 0 and standard deviation of 1. Let mean(X) denote the arithmetic mean of X and std (X) denote the standard deviation of X, then the formula for z-score normalization is

$$x' = \frac{\mathrm{x} - \mathrm{mean(x)}}{\mathrm{std\ (x)}} \qquad (3.18)$$

3.5.3 Tanh-estimators normalization

This normalization is based on Hampel estimators [95] and is given by

$$x' = \frac{1}{2}\left\{\tanh\left(\mathrm{k}\left(\frac{\mathrm{x} - \mathrm{mean(S')}}{\mathrm{std\ (S')}}\right)\right) + 1\right\} \qquad (3.19)$$

The parameter k is a constant whose value depends on the standard deviation of given data. In Eq. (18), mean (S') denotes the mean and std (S') denotes the standard deviation of the raw data as given by Hampel estimators.

3.6 Overview

In the very first part of the implementation, we shall deal with the problem of dimensionality reduction because the image of iris consists of many numbers of features. Since in every iris there are few features which give a unique identity to every person, so these features can be decomposed with help of Principal component analysis which is a widely used mathematical tool that uses an orthogonal transformation to reduce a set of similar or correlated component into a set of linearly uncorrelated components. The next part shall deal with extraction of features such as striations, pits, collagenous fibers etc. of the iris using the Independent Component Analysis (ICA) algorithm using Kurtosis method, which is a another mathematical tool developed to determine a linear internal representation of non Gaussian data so that the above fetched set components are statistically autonomous or independent to each other. The implementation of this algorithm is done with the help of MATLAB.

3.7 Dimensionality Reduction Techniques

Estimating ICA in the original, high-dimensional space may lead to poor results. For e.g., most of the independent sources may contain only noise.

3.7.1 Principle Component Analysis

The technique that is best suited in the mean- square error sense and a linear dimension reduction is the Principal component analysis (PCA) [96, 97]. It is second-order method since it is based on the covariance matrix of the variables. In various fields, it is also known as the singular value decomposition (SVD), the Karhunen-Loμ eve transform, the Hotelling transform, and the empirical orthogonal function (EOF) method. In principle, the main aim of PCA is to reduce the dimension of the data by finding a few orthogonal linear combinations (the PCs) of the original variables with the largest variance.

To discuss in detail, in principal component analysis (PCA), an observed vector x is first centered by removing its mean (in practice, the mean is estimated as the average value of the vector in a sample). Then the vector is transformed by a linear transformation into a new vector, possibly of lower dimension, whose elements are uncorrelated with each other. The linear transformation is found by computing the eigen value decomposition of the covariance matrix. For a zero-mean vector x, with n elements, the covariance matrix C_x is given by:

$$Cx = E\{xx^T\} = EDE^T \qquad (3.20)$$

Where $E = (e_1, e_2, \ldots, e_n)$ =orthogonal matrix of eigenvectors of C_x

D= diag ($\lambda 1, \lambda 2, \ldots, \lambda n$) = diagonal matrix of eigen value of C_x

Whitening or sphering can be described as $z = Px$ (3.21)

Where P is the whitening matrix and z is a new matrix that is white.

P is defined as $P = D^{-1/2} * E^T$ (3.22)

Subsequent ICA estimation is done on z instead of x. For whitened data it is enough to find an orthogonal demixing matrix if the independent components are also assumed white [93].

3.7.2 Random projection

Other than PCA, random projection (RP) is also a highly used technique for dimensionality reduction [98, 99, 100]. The most important property of the RP method is that it is a general data reduction method which does not depend on a particular training data set. Also, unlike Discrete Cosine Transform (DCT) or Discrete Fourier Transform (DFT) its basis vectors do not exhibit particular frequency or phase properties.

In this method, the original data which is high dimensional is projected onto a low-dimensional subspace using a random matrix, whose columns have unit length. Unlike PCA, which computes the low uncorrelated data by optimizing a particular criteria (e.g., PCA finds a subspace that maximizes the variance in the data), RP does not use such criteria, therefore, it is data independent. Also, it represents computationally simple and effective method that upholds the structure of the data without significant distortion [101]. Few theoretical outcomes prove that RP preserves for example volumes and affine distances [102] or the structure of data (e.g., clustering) [103].

3.8 ICA Algorithm (Fast ICA)

In the previous sections, we introduced different measures of nongaussianity, i.e. objective functions for ICA estimation. In this section, we shall introduce an effective method of maximization suited for this task. It is here assumed that the data is preprocessed by centering and whitening as discussed in the preceding section of dimensionality reduction. We have used the PCA technique to obtain the whitening matrix and the whitened vector.

3.8.1 Fast ICA for one unit

Assume that we have collected a sample of the sphere (or whitened) random vector z, which is in case of blind source separation, is a collection of linear mixture of independent source signals. The basic method of Fast ICA algorithm is as follows:

1. Take a random initial row vector w(0) from the prewhitening matrix P
2. Let $w^T(k) = E\{z [z^T * w^T (k-1)]^3\} - 3 w^T(k-1)$
3. Divide w(k) by its normalization
4. If $| w(k)*w^T(k-1) |$ is not close to 1, let k=k+1 and go to step 2. Otherwise the algo is convergent and outputs w(k)

Final vector w(k) equals one of the rows of the orthogonal demixing matrix P. w(k) separates one of the nongaussian source signals→ w(k)*z(t) t=1,2,.. equals one of the source signals.

3.8.2 Fast ICA for several units

For estimating n independent components, run these algorithm n times. To assure the estimation of different independent sources each time, an orthogonalizing projection is added inside the loop. The column of the demixing matrix P is orthonormal because of the sphering. This way each of the independent components are estimated by projecting the current solution w(k) on the space orthogonal to the columns of the demixing matrix P previously found. Define the matrix P as the matrix whose rows are the previously found rows of P. Then, the projection operation is added in the beginning of step 3.

3. $w = w - P^* proj(P)^T * w$, then Divide w(k) by its normalization.

Similarly, the initial row vector should be projected this way before starting the iterations. To prevent estimation error in proj(P) from deteriorating the estimate w(k), this projection step can be omitted after the first few iterations: once the solution w(k) has entered the basin of attraction of one of the fixed points, it will stay there and converge to that fixed point.

3.9 Properties of Fast ICA Algorithm

The FastICA algorithm has a number of desirable properties when compared with existing methods for ICA.

1. The very first and essential property of the ICA is that the signal components to which the ICA will be applied should be cubically converging in nature. If these components are not cubically converging in nature then they must be at least quadratically converging in nature [104]. These are in contrast to ordinary ICA algorithms which are based on (random) gradient descen methods, where the convergence is only linear. Hence it depicts that a very fast convergence can be confirmed by using ICA on variety of data either by simulation or on real time experimental data [105].
2. Unlike the gradient-based algorithms, it is not possible to choose step size parameter. This property of the ICA makes it preferable in the sense that it is easy to be applied in a wide range of applications.

3. This algorithm determines the uncorrelated components that have non Gaussian distribution. The ICA is different from other algorithms in sense that it requires availability of probability density function so that nonlinearity must be chosen.
4. The optimization of the system's performance depends upon the chosen nonlinearity. By this the system becomes robust and of minimum variance [104].
5. As in the projection pursuit, the uncorrelated (independent) components can be figured one by one. This helps in exploratory data analysis, and decreases the computational load of the method in cases where only some of the independent components need to be estimated.
6. The FASTICA method is advantageous in the neural algorithm as it is parallel, distributed, computationally simple, and requires little memory space. Stochastic gradient methods seem to be preferable only if fast adaptivity in a changing environment is required [90].

3.10 Applications of ICA

Various applications of ICA algorithm include image processing, communications, biomedical, audio, and sensor array signal processing [91].

3.10.1 Image processing

In the field of remote sensing the image distribution into various classes or categories of the same type has been one of the most recent and important task that must be settled. Furthermore, in the field of automatic classification of the image sensing, number of scholarly person has been exploring various terminologies which are fast, efficient and highly precise in nature. Since the demands of above mentioned classes of novel categories are increasing in number, the chances of false classification are also increasing day by day. An interesting fact about classification is that if we could filter out certain characteristic or the features of image pixels beforehand out of thousands features, and then on the basis of remaining pixels classification, we can cut down the chances of errors efficaciously and can accelerate the classification process.

The favorable position of the image change detection has been utilized in many applications and has evidenced in numerous views of international economy. A concerning fact is that the image change detection has become a sensational issue in the world of remote sensing

technologies. But the process of remote sensing has always been a critical task due to its complex structure, therefore, there no such a method that is united into a whole for accurate image change detection. Recently available methods work on numerous images preprocesses independently, and their inter operability limits the ability and accuracy to observe changes in image. Conventionally, some feature decomposition tools like PCA & difference and ratio transformation helps to some extent to achieve an appreciable degree of accuracy even though they require some duplicated trials to pick out a doorway for pixels change detection.

Along with other decomposition terminologies, Independent Component Analysis (ICA) is also emerging as one of the effective methodologies which help in solving blind source separation problem. In ICA we attempt to separate out the correlated elements or feature and find some uncorrelated component called independent component. ICA is a statistical and mathematical approach for bringing out concealed elements that underlie sets of stochastic variable, measurements phenomena, or indicates. In order to uncorrelated the multiple input signals ICA uses highly advanced statistics by making the result signals independent from each other. While ICA in biometric applications becoming more popular, it is also practiced in error detection, biomedicine signal processing (EEG & ECG), feature extraction, sound signal detachment etc. Although ICA mainly used for signal processing but its use in remote sensing image processing, is comparatively to a lesser extent [106].

3.10.2 Feature Extraction by ICA

In the earlier time, the mathematical models for signal processing were used to develop around the fundamental principle of statistical generative complex entity of the detected signals. In these models the observed data is converted in to a new data type to give a new representation of the data. Next, the new data type is then used to complete the task of data decomposition, error correction, feature extraction and pattern recognition. The generative model has given its useful contribution in areas like neuro-science, which ultimately utilized to simulate the attributes of neurons in principal sensory areas.

The process of feature extraction includes definite course of signals used to a great degree and are obtained from raw pictures. These sources of raw images and scenes come across in our daily lives all the time; such as images of wild-life views, human living surroundings, animations etc. The source images obtained from these surroundings depicts to a similar category, therefore an identical statistical model can be developed for the homogeneous data

type employing reflections of these signals. In addition to this, the developed model can be used to perform the operations like data decomposition and error detection, error correction.

As an alternative, the use of independent component analysis (ICA) to develop an instinctive model for natural images is one of the favored choices. ICA not only offers the most advanced model for low level images representation in the field of image processing but also widely accepted at research fronts.

As it is mentioned earlier that, ICA is an independent features extraction tool which extract information from multiple number of data. The application of ICA requires some assumptions such as, it works for a multidimensional data so that a moving window can be prepared to fetch out the independent information from the data to which the ICA is applied the working principle of ICA closely resembles to sparse coding in which only those features are extracted which are simultaneously active in a lesser quantity. The process of Feature extraction in sparse based model is achieved with the help of wavelets or Gabor analysis because this method gives a better result for closely related feature decomposition of natural images. Next, the features obtained after decomposition of the image are restricted in space as well as in frequency, and are adjusted or located in relation to surroundings or circumstances. The features with these characteristics are best suited for the image processing.

The application of ICA is not limited to any certain area. At one hand, if the linear feature of an image can be extracted by ICA, the more advance approach of ICA can be used to prevail nonlinear features too. In addition to this, Independent subspace analysis contributes to find features with invariability and is insensitive to location and phase change. One more effective branch of the ICA used for topographic analysis is the topographic ICA, which helps is demonstrating topographical features of the signals. This method is also shows the effective invariance with different operating condition. Along with these methods, wavelet or Gabor coefficients have been enquired in to establish a model to determine the high order correlation between the independent components. The versatility of the ICA framework can be observed from different research work done on different data such as color and stereo images hyperspectral data, video data and audio data. [109]

3.10.3 Brain imaging Applications

The brain is one of the most complex anatomical structural models that persists indefinite number of signal and information. With the advancement in the field of anatomical study now it is possible to collect the immense quantity of information with the help of novel anatomical and operational brain imaging technologies. Therefore, it has become very significant to draw out the all important characteristics from the information to permit an easier representation or interpretation of the behavior. The complexity of the operation of fetching important information has made independent component analysis ICA a very promising tool. Furthermore, the popularity of ICA for complex operation has opened the gate for other image processing areas too. ICA is giving its services to application such as electroencephalograms (EEG) and magnetoencephalograms (MEG), which are transcription of the electrically and magnetically generated signal from the neural currents within the brain.

3.10.4 Telecommunications

In the serialized set of innovative and emerging application of ICA, telecommunications is the new area in which ICA has shown great possiblities. In the field of telecommunication (Ristaniemi and Joutsensalo 1999) has employed blind source separation techniques where ICA has given its useful contribution in the separation of the one user's signal from multiple number of other users' signals in CDMA mobile communications. Although ICA is known for blind source separation but the problem of distinguishing one user's signal from others is considered as semi-blind because a certain amount of information is available earlier in time on the CDMA data model. But for the convenience of multiple parameter estimation ICA is highly suitable because previously available information about the communication system provide aclear performance betterment over conventional approximation proficiencies.

3.10.5 Time series prediction by ICA

It is clear from our previous discussions that the transformation of the source data through ICA inclines to develop component signals. This component signal can be decomposed with lesser bits than the actual signals. The component signals thus obtained are more compact, more integrated and steady in nature. With the availability of component signal one can efforts to anticipate the blind signals which is mixed with the original signal. One of the approach suggested that blind source separation can be achieved first by attending the ICA

space, anticipating the component there, and then transforming back to the actual statistic. Relying upon the different time systems of the different methods the process of anticipation can be exercised individually and with different algorithms for each component. This system requires the user's attention for the overall components anticipation procedure. Another facility that can be added to the system is that it can be formulated with ICA contrast function to make the system robust against the anticipation errors.

3.10.7 Audio separation

There have also been a number of other interesting applications and blind source separation for audio signal is one of them. Very often, in real world problems, recording the sound of multiple numbers of people simultaneously do not demonstrate uniform intensities. The main goal behind procedure is to separate the voice of just one of the source out of multiple sources which may have recorded with microphone in a public event. One interesting fact about recorded voice is that, only one person was addressing to the microphone and all the other sources can be considered as noise. So the blind source separation has to deal with problem of noise reduction or noise removal.

For this purpose an additive (linear) filter or possibly more advanced proficiencies like wavelet and sparse code can be used to cancel the noise from the original signal. Although, the use of above motioned techniques help to reduce the noise, but their performance are unsatisfactory. These systems can work well under certain circumstances i.e. noise should have spectral features that are distinctly unlike from voice signal. The problem of using multiple microphones for effective noise removal can be replaced by estimating the source blindly. For this reason, an ICA model is used, and the problem is considered as blind source separation.

Chapter 4

Results and Discussions

4.1 Overview

Various steps have been used to develop an iris based biometric recognition system. These steps are:

1. Capture an iris image/ obtain it from database
2. Segmentation
3. Dimensionality reduction (preprocessing)
    - centering
    - whitening
4. Feature extraction (using ICA)
5. Matching and validation

4.2 Database

Iris images of CASIA-Iris-Interval were captured with CASIA's self-developed close-up iris camera. The most compelling feature of their iris camera is that they have designed a circular NIR LED array, with suitable luminous flux for iris imaging. Because of this novel design, their iris camera can capture very clear iris images. CASIA-Iris-Interval is well-suited for studying the detailed texture features of iris images [110]. From this database, 10 images (5 left eyes and 5 right eyes) of 20 users are collected. In Figure 4.1, a single user's 10 input images (5 left & 5 right images) are shown.

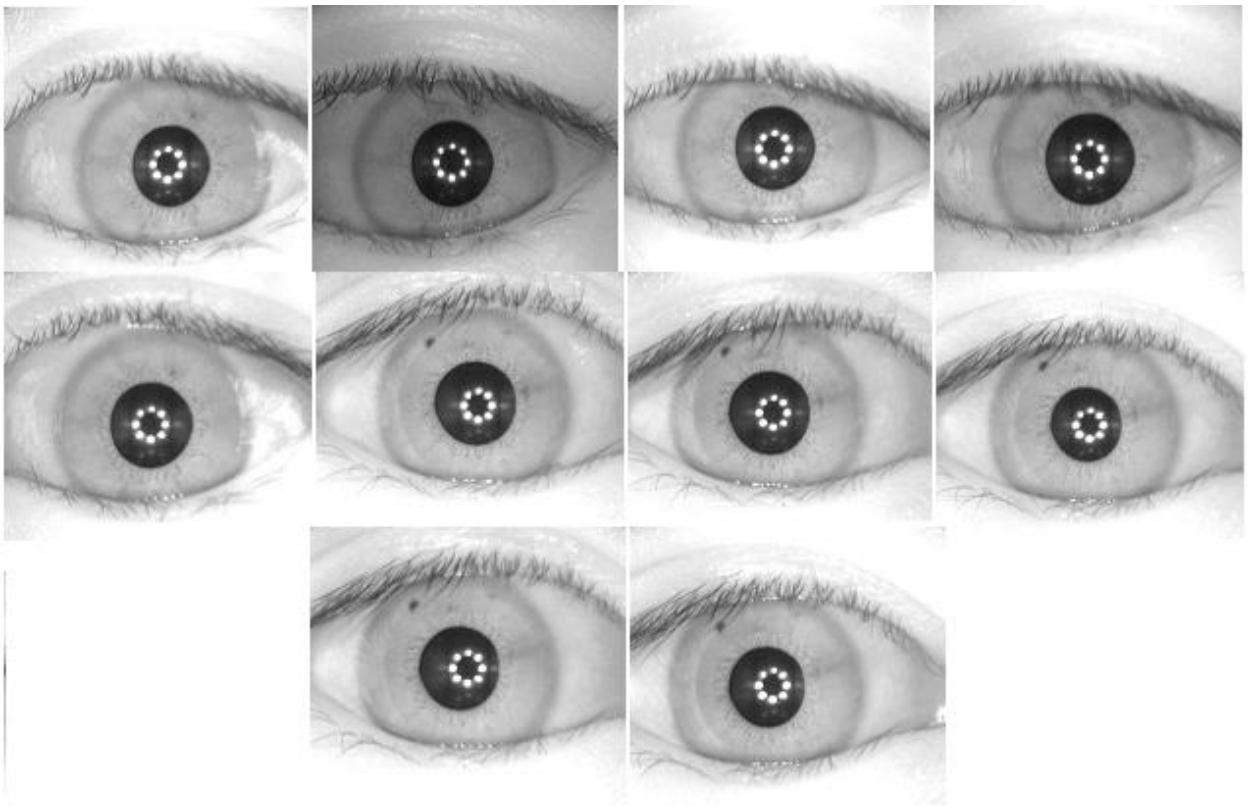

Figure 4.1: Single user's 10 images (5 left & 5 right images)

4.3 Input image

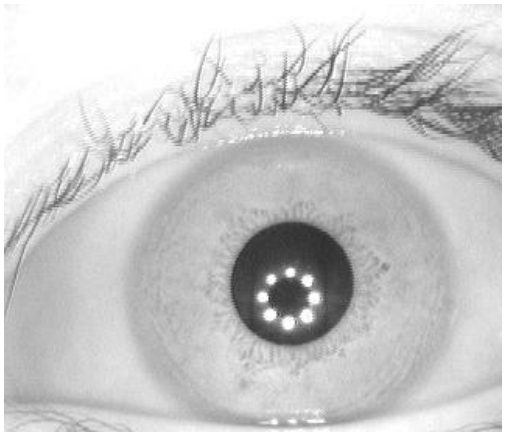

Figure 4.2: Input image

An input image is shown in Figure 4.2 that has been taken from the database discussed in section 4.2. The ICA algorithm will be applied on this input image after its segmentation and pre processing and then the features shall be extracted.

4.4 Segmentation

A good segmentation approach is that which can extract useful iris information from noisy iris images. This is a crucial step to be done before any algorithm is applied. Consequently, the focus of our work is first placed on the development of a robust segmentation approach that can overcome such unpredictable noise effects in order to secure recognition outcomes with high accuracy. The flowchart shown in Figure 4.3 reflects the steps followed in segmentation process.

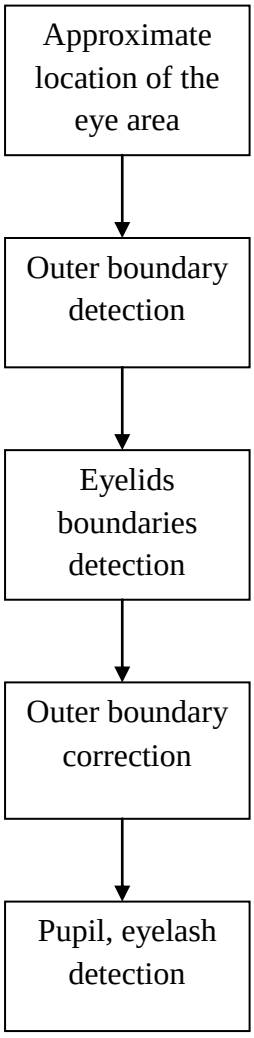

Figure 4.3: Flowchart of segmentation process

Figure 4.4 shows the image when segmentation is done on input image 4.2. Further, the iris region can be extracted out of the segmented image as shown in Figure 4.5. The dimensions of the segmented image obtained are 100*100.

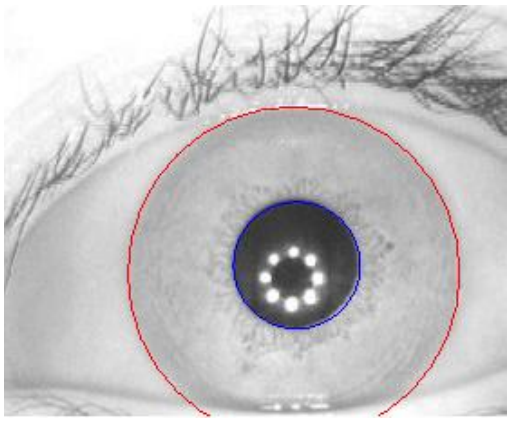

Figure 4.4: Segmented Image

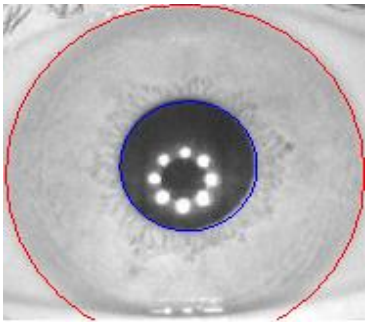

Figure 4.5: Extraction of iris region

Similarly, all the images in the database are segmented to extract the limbic and pupillary regions to be further pre processed for the feature extraction. Figure 4.6 shows the segmented images of the database shown in Figure 4.1.

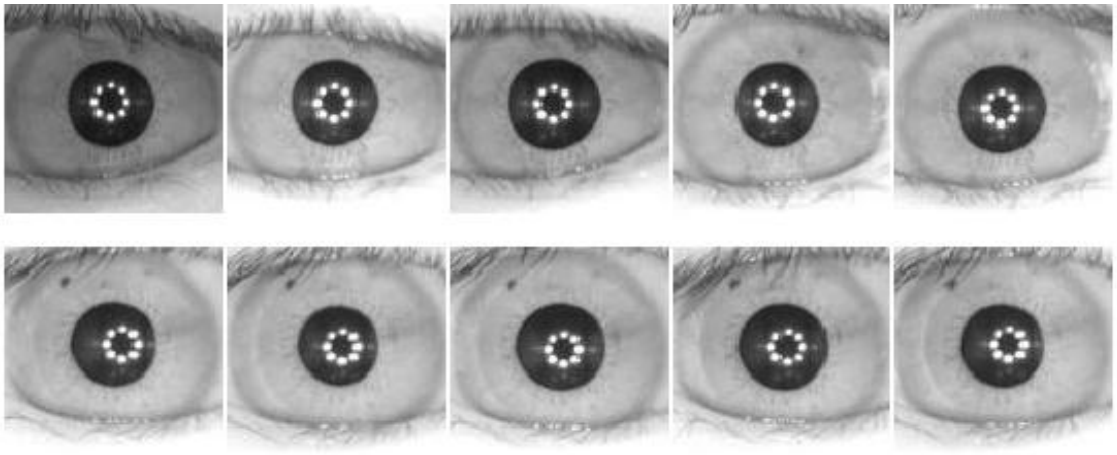

Figure 4.6: Corresponding segmented images of input images in database 4.1.

4.5 Dimensionality Reduction

Once the segmented image is obtained, we shall reduce its dimensions and follow the following steps:

Step1: Centering: Subtract the mean vector m=E{x} from the input vector of the image. A zero mean vector is formed eventually. Figure 4.7 shows the image after its centering.

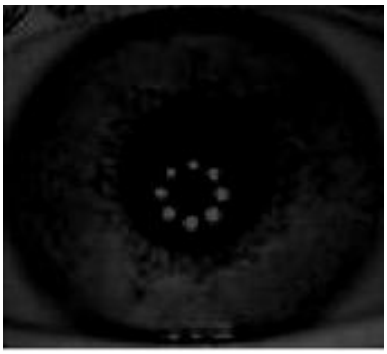

Figure 4.7: Image after centering

Step2: Whitening: We will transform the observed vector x (zero mean vector) linearly, to obtain a new vector z which is white; i.e. the components are uncorrelated and their variances equal unity.

- For whitening: Use of covariance matrix-

$$C_x=E\{xx^T\}$$

x=zero mean vector

100*100 values of covariance matrix are created out of which 500 are shown through tables 4.1 to 4.5.

Table 4.1: First 100(1-100) values of covariance matrix

4.91E+08	2.71E+08	2.14E+08	74720676	49657097	74297531	2.04E+08	2.45E+08	4.31E+08	4.27E+08
3.26E+08	2.94E+08	2.05E+08	74693594	38321594	53215219	2.35E+08	2.57E+08	4.46E+08	4.08E+08
2.69E+08	2.96E+08	1.92E+08	70746842	40839281	59544665	2.48E+08	2.57E+08	4.33E+08	4.2E+08
2.59E+08	2.82E+08	1.84E+08	63120126	32871728	93030489	2.01E+08	2.59E+08	4.15E+08	3.91E+08
2.5E+08	2.75E+08	1.82E+08	49253103	32938031	1.58E+08	1.87E+08	2.88E+08	4.25E+08	3.44E+08
2.42E+08	2.76E+08	1.38E+08	49729886	58703846	1.75E+08	1.65E+08	3.19E+08	4.29E+08	4.24E+08

2.29E+08	2.64E+08	1.18E+08	53704383	94405646	1.31E+08	1.76E+08	3.42E+08	4.32E+08	5.89E+08
2.25E+08	2.62E+08	95970226	50212662	88462928	84953587	1.94E+08	3.67E+08	4.46E+08	5.69E+08
2.18E+08	2.51E+08	83753295	43851574	1.1E+08	98698152	1.98E+08	3.95E+08	4.59E+08	7.94E+08
2.42E+08	2.29E+08	80234952	46488875	1.07E+08	1.57E+08	2.16E+08	4.16E+08	4.52E+08	1.09E+09

Table 4.2: Next 100(101-200) values of covariance matrix

3.26E+08	1.85E+08	1.43E+08	51735288	36480953	44543795	1.26E+08	1.73E+08	2.73E+08	2.74E+08
2.31E+08	1.99E+08	1.35E+08	52119273	28534075	37572342	1.45E+08	1.79E+08	2.81E+08	2.61E+08
1.96E+08	2E+08	1.27E+08	49923928	30532538	43118241	1.55E+08	1.76E+08	2.73E+08	2.62E+08
1.89E+08	1.91E+08	1.21E+08	45025956	24647345	62475686	1.33E+08	1.75E+08	2.64E+08	2.43E+08
1.83E+08	1.85E+08	1.19E+08	35530501	24589613	97389805	1.26E+08	1.92E+08	2.72E+08	2.25E+08
1.8E+08	1.86E+08	91492337	35859431	41867938	1.08E+08	1.16E+08	2.12E+08	2.75E+08	2.83E+08
1.7E+08	1.78E+08	78579038	38698503	61651951	84762657	1.27E+08	2.25E+08	2.78E+08	3.91E+08
1.65E+08	1.76E+08	65444941	36299059	57283223	60656830	1.4E+08	2.38E+08	2.87E+08	4.04E+08
1.59E+08	1.68E+08	56716036	31847811	63343965	71789521	1.42E+08	2.52E+08	2.96E+08	5.58E+08
1.71E+08	1.54E+08	54251734	33924485	60698218	1.02E+08	1.55E+08	2.63E+08	2.93E+08	7.27E+08

Table 4.3: Next 100(201-300) values of covariance matrix

2.69E+08	1.71E+08	1.25E+08	43433637	32284259	38148390	1.05E+08	1.43E+08	1.43E+08	2.32E+08
1.96E+08	1.81E+08	1.17E+08	43688348	25527412	34619891	1.2E+08	1.47E+08	1.47E+08	2.22E+08
1.73E+08	1.82E+08	1.08E+08	42080563	26540977	39892307	1.28E+08	1.43E+08	1.43E+08	2.22E+08
1.71E+08	1.75E+08	1.03E+08	37598004	21413535	54231688	1.13E+08	1.42E+08	1.42E+08	2.1E+08
1.69E+08	1.69E+08	99111519	30117285	22323534	78249747	1.07E+08	1.55E+08	1.55E+08	2.06E+08
1.68E+08	1.68E+08	78018219	30590616	37215665	86910727	99586273	1.7E+08	1.7E+08	2.61E+08
1.6E+08	1.59E+08	67237864	32742838	53401572	70667122	1.08E+08	1.8E+08	1.8E+08	3.53E+08
1.57E+08	1.57E+08	56288813	30685715	51085791	53795906	1.18E+08	1.9E+08	1.9E+08	3.72E+08
1.51E+08	1.49E+08	48262115	27485776	51975546	63223420	1.2E+08	2.01E+08	2.01E+08	4.93E+08
1.6E+08	1.36E+08	45425910	29564492	49217344	85793578	1.3E+08	2.09E+08	2.09E+08	6.17E+08

Table 4.4: Next 100(301-400) values of covariance matrix

2.59E+08	1.8E+08	1.26E+08	41323536	32911207	39799617	1.06E+08	1.36E+08	2.06E+08	2.29E+08
1.89E+08	1.89E+08	1.17E+08	41481921	26376353	36923464	1.21E+08	1.38E+08	2.12E+08	2.21E+08
1.71E+08	1.9E+08	1.07E+08	40224577	26681067	42422588	1.28E+08	1.34E+08	2.09E+08	2.24E+08
1.75E+08	1.82E+08	99981804	35635905	21377098	56224993	1.12E+08	1.34E+08	2.07E+08	2.17E+08
1.79E+08	1.76E+08	95638242	29141339	23223580	78510561	1.06E+08	1.45E+08	2.17E+08	2.2E+08

1.78E+08	1.74E+08	76462635	29830356	38093107	87309697	98845787	1.59E+08	2.22E+08	2.79E+08
1.7E+08	1.64E+08	65733983	31572376	54125711	72355025	1.06E+08	1.68E+08	2.27E+08	3.73E+08
1.68E+08	1.6E+08	54810931	29533287	53500868	55757166	1.14E+08	1.78E+08	2.35E+08	3.92E+08
1.61E+08	1.51E+08	46763771	27193935	52887910	64229793	1.16E+08	1.88E+08	2.45E+08	5.03E+08
1.71E+08	1.37E+08	43463773	29636654	49917102	86365790	1.25E+08	1.96E+08	2.43E+08	6.14E+08

Table 4.5: Next 100 (401-500)values of covariance matrix

2.5E+08	1.89E+08	1.23E+08	38328457	33628975	40350535	1.05E+08	1.28E+08	1.89E+08	2.22E+08
1.83E+08	1.95E+08	1.13E+08	38387582	27530963	39066962	1.18E+08	1.28E+08	1.94E+08	2.15E+08
1.69E+08	1.96E+08	1.02E+08	37646618	27153485	44882113	1.24E+08	1.24E+08	1.92E+08	2.2E+08
1.79E+08	1.88E+08	95059063	33162467	21614369	57804731	1.1E+08	1.24E+08	1.94E+08	2.17E+08
1.88E+08	1.8E+08	89823677	27893321	24410642	77777360	1.03E+08	1.33E+08	2.05E+08	2.28E+08
1.9E+08	1.78E+08	72894569	28849351	38897008	86640306	97378738	1.45E+08	2.11E+08	2.92E+08
1.83E+08	1.64E+08	62515477	30152880	53875722	73810365	1.03E+08	1.54E+08	2.16E+08	3.87E+08
1.8E+08	1.59E+08	52046795	28183942	54967254	57723409	1.1E+08	1.63E+08	2.25E+08	4.09E+08
1.74E+08	1.49E+08	44133870	26827989	52034366	65125299	1.12E+08	1.72E+08	2.35E+08	5.09E+08
1.82E+08	1.35E+08	40469906	29772437	48638125	85414438	1.19E+08	1.79E+08	2.34E+08	6.04E+08

Step 3: Method for whitening: Eigen value-decomposition of covariance matrix

$$C_x=E\{xx^T\}=EDE^T$$

where, E→ orthogonal matrix of Eigen vectors of C_x and D→ diagonal matrix of its Eigen values.

Step 4: To obtain whitening matrix: z=Px

where, z→ whitened matrix and P→ whitening matrix

$$P= D^{(-1/2)}* E^T$$

Figure 4.8 and 4.9 shows the whitening matrix (P) and whitened matrix (z) respectively.

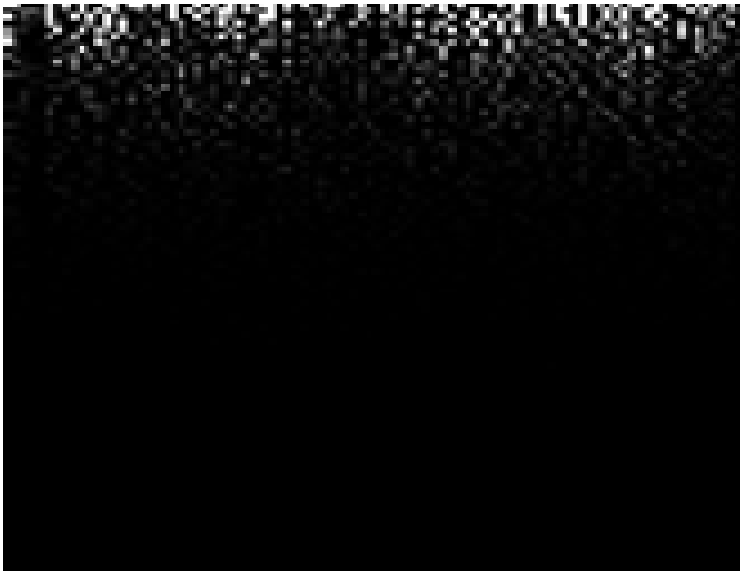

Figure 4.8: Whitening matrix P

Figure 4.9: Whitened matrix z

4.6 ICA Algorithm

Step 1: Take a initial row vector w (0), let k=1

Step 2: Let $w^T(k)=E\{z[z^T*w^T(k-1)]^3\}-3*w^T(k-1)$

Step 3: Normalize total matrix obtained after the above iterations

Normalization= (ww-mean)/ std

where, std is the standard deviation

Step 4: If abs[w(k)* w^T(k-1)] is not close enough to 1, let k=k+1. Otherwise algo is convergent and outputs w(k). w(k) separates one of the non-gaussian source.

Table 4.6 is obtained after all the above steps. In this table, the value that will be close to 1 shall signify the independent component.

Table 4.6: convergent matrix containing single source of independent component

0.002658	0.002658	0.002658	0.002658	0.002658	0.002658	0.002658	0.002658	0.002658
0.002658	0.002658	0.002658	0.002658	0.002658	0.002658	0.002658	0.002658	0.002658
0.002658	0.002658	0.002658	0.002658	0.002658	0.002658	0.002658	0.002658	0.002658
0.002658	0.002658	0.002658	0.002658	0.002658	0.002658	0.002658	0.002658	0.002658
0.002658	0.002658	0.002658	0.002658	0.002658	0.002658	0.002658	0.002658	0.002658
0.002658	0.002658	0.002658	0.002658	0.002658	0.002658	0.002658	0.002658	0.002658
0.002658	0.002658	0.002658	0.002658	0.002658	0.002658	0.002658	0.002658	0.002658
0.002658	0.002658	0.002658	0.002658	0.002658	0.002658	0.002658	0.002658	0.002658
0.002658	0.002658	0.002658	0.002658	0.002659	0.002658	0.002659	0.002653	0.002656
0.002502	0.001641	0.007679	0.086841	0.813458	7.310531	65.91162	592.9391	5337.333

Step 5: The above steps were for single source. Repeat these steps for n sources, by taking the different initial row vectors of the whitening matrix P as in step 1. Different column vectors are generated containing the different values; we need to find those whose values that will converge to 1.

Step 6: A template is now created so as to separate all the converging values (near to one) from the multiple numbers of the unconverging data, obtained after step 5. Table 4.7 will show the n independent source values obtained after all above steps.

Table 4.7: convergent matrix containing n independent components (sources) of an image

0.813457872	0.777096381	0.752853806	0.881417021	0.779841248	0.688293183
0.812966146	0.666726416	0.920471582	0.896807568	0.974419066	0.897321483
0.839948483	0.759010456	0.110217838	0.9061055	0.890159296	0.890479823
0.878729731	0.835775095	0.897587227	0.781274992	0.875782983	0.965681523
0.126968623	0.804367854	0.769427198	0.911939826	0.894062959	0.920371847
0.112289755	0.119752078	0.820034935	0.126460883	0.856710505	0.124363615
0.862086159	0.89388191	0.113572297	0.871260182	0.141046912	0.858430471

0.124879373	0.902068382	0.836550694	0.105927324	0.913407471	0.870013675
0.942693644	0.949860829	0.115985121	0.937157005	0.912053095	0.12223436
0.961055424	0.886856107	0.89731158	0.878945005	0.91984609	0.112122455
0.919558231	0.113705898	0.798902789	0.113396906	0.942684372	0.894616161
0.110857443	0.1132463	0.915172933	0.99117406	0.972039733	0.839478593
0.109524276	0.892176613	0.874808566	0.952034479	0.126517587	0.114717107
0.682791868	0.113590702	0.866880465	0.968948747	0.109093987	0.419994252
0.483925505	0.483925505	0.421956005	0.820276959	0.081887966	0.468765321

4.7 Matching

4.7.1 Database and real time data creation

The process of matching starts with the database formation by obtaining the independent component sources for multiple images, one by one. Here, we have shown the creation of the database on the basis of ICA. For the same reason we have taken four images of a user, two of left eye and two of right. The tables 4.8 and 4.9 show the ICA sources for two left eye images of the same user and tables 4.10 and 4.11 for right eye.

Table 4.8: Templates obtained from n independent sources of User 1 image1(left iris image)

0.784	0.848	0.127	0.127	0.121	0.125	0.123	0.951	0.136	0.128
0.822	0.874	0.114	0.114	0.143	0.114	0.121	0.896	0.973	0.984
0.779	0.770	0.152	0.152	0.128	0.136	0.932	0.100	0.114	0.970
0.800	0.978	0.116	0.116	0.123	0.139	0.105	0.113	0.925	0.918
0.838	0.131	0.916	0.916	0.980	0.127	0.098	0.137	0.117	0.037
0.768	0.990	0.130	0.130	0.110	0.122	0.119	0.909	0.837	0.892
0.902	0.113	0.121	0.121	0.144	0.126	0.104	0.103	0.856	0.114
0.893	0.120	0.133	0.133	0.106	0.095	0.137	0.152	0.129	0.104
0.921	0.110	0.138	0.138	0.123	0.118	0.121	0.934	0.001	0.808
0.797	0.119	0.124	0.124	0.130	0.117	0.912	0.093	0.027	0.866

Table 4.9: Templates obtained from n independent sources of User 1 image2 (left iris image)

0.701	0.897	0.129	0.131	0.135	0.143	0.103	0.098	0.005	0.109
0.825	0.985	0.113	0.854	0.149	0.132	0.125	0.124	0.773	0.893
0.963	0.852	0.858	0.130	0.122	0.970	0.124	0.142	0.126	0.760
0.943	0.114	0.968	0.120	0.120	0.118	0.113	0.111	0.840	0.125
0.906	0.910	0.993	0.133	0.131	0.130	0.140	0.128	0.118	0.065

0.943	0.947	0.135	0.138	0.143	0.123	0.139	0.104	0.783	0.142
0.924	0.972	0.130	0.878	0.122	0.111	0.130	0.111	0.008	0.111
0.928	0.977	0.131	0.122	0.117	0.148	0.951	0.120	0.730	0.134
0.112	0.143	0.133	0.126	0.980	0.112	0.147	0.117	0.057	0.866
0.846	0.115	0.975	0.121	0.105	0.134	0.136	0.955	0.075	0.977

Table 4.10: Templates obtained from n independent sources of User 1 image6 (right iris image)

0.736	0.111	0.113	0.128	0.116	0.172	0.114	0.124	0.129	0.898
0.829	0.125	0.908	0.121	0.130	0.127	0.126	0.120	0.080	0.728
0.917	0.940	0.118	0.129	0.116	0.949	0.987	0.149	0.091	0.751
0.798	0.983	0.136	0.134	0.110	0.120	0.132	0.133	0.799	0.148
0.831	0.139	0.126	0.131	0.143	0.128	0.111	0.138	0.957	0.757
0.133	0.116	0.123	0.142	0.116	0.122	0.128	0.977	0.116	0.120
0.738	0.122	0.122	0.938	0.133	0.110	0.125	0.982	0.836	0.131
0.855	0.894	0.135	0.133	0.140	0.143	0.126	0.102	0.875	0.115
0.954	0.130	0.117	0.113	0.118	0.127	0.978	0.912	0.850	0.087
0.970	0.951	0.925	0.143	0.135	0.127	0.134	0.132	0.909	0.922

Table 4.11: Templates obtained from n independent sources of User 1 image7 (right iris image)

0.965	0.981	0.130	0.120	0.122	0.956	0.146	0.130	0.065	0.908
0.791	0.868	0.113	0.994	0.105	0.120	0.133	0.971	0.116	0.050
0.833	0.895	0.118	0.119	0.111	0.119	0.117	0.886	0.108	0.827
0.888	0.976	0.124	0.117	0.135	0.146	0.123	0.102	0.958	0.817
0.116	0.938	0.116	0.096	0.145	0.110	0.115	0.999	0.123	0.129
0.920	0.896	0.108	0.135	0.951	0.115	0.124	0.116	0.899	0.010
0.799	0.939	0.143	0.130	0.135	0.125	0.121	0.957	0.832	0.084
0.123	0.127	0.128	0.966	0.115	0.112	0.096	0.107	0.118	0.880
0.766	0.938	0.124	0.125	0.122	0.115	0.900	0.110	0.817	0.901
0.941	0.979	0.120	0.144	0.116	0.128	0.121	0.108	0.728	0.827

Once the database is formed, we shall collect the real time images which shall contain the n independent sources of the same user, but different images apart from those collected for the database. The tables 4.12, 4.13 and 4.14 show the ICA sources for left eye images of the same user while 4.15, 4.16 and 4.17 for right eye.

Table 4.12: Real time data obtained from n independent sources of User 1 image3 (left iris image)

0.115	0.910	0.119	0.134	0.894	0.125	0.132	0.121	0.123	0.114
0.116	0.995	0.933	0.888	0.122	0.133	0.123	0.120	0.117	0.885
0.799	0.112	0.133	0.146	0.113	0.114	0.133	0.114	0.117	0.778
0.794	0.976	0.129	0.118	0.124	0.145	0.136	0.118	0.869	0.133
0.803	0.986	0.118	0.140	0.137	0.126	0.114	0.891	0.939	0.062
0.966	0.120	0.122	0.120	0.124	0.130	0.133	0.136	0.829	0.000
0.844	0.123	0.130	0.126	0.127	0.125	0.149	0.123	0.112	0.111
0.133	0.114	0.131	0.126	0.119	0.125	0.936	0.119	0.128	0.991
0.910	0.955	0.128	0.127	0.134	0.115	0.139	0.111	0.135	0.792
0.114	0.123	0.125	0.125	0.127	0.122	0.118	0.119	0.093	0.919

Table 4.13: Real time data obtained from n independent sources of User 1 image4 (left iris image)

0.999	0.877	0.137	0.151	0.136	0.119	0.972	0.126	0.116	0.962
0.115	0.952	0.989	0.136	0.129	0.123	0.126	0.123	0.112	0.916
0.133	0.803	0.116	0.129	0.114	0.145	0.125	0.118	0.982	0.117
0.851	0.995	0.126	0.142	0.129	0.161	0.135	0.958	0.154	0.688
0.865	0.948	0.119	0.134	0.130	0.157	0.106	0.995	0.127	0.769
0.128	0.126	0.919	0.113	0.146	0.144	0.134	0.119	0.081	0.095
0.975	0.961	0.148	0.134	0.134	0.119	0.987	0.128	0.127	0.114
0.124	0.970	0.124	0.124	0.118	0.154	0.151	0.136	0.123	0.165
0.844	0.115	0.124	0.125	0.148	0.163	0.118	0.117	0.006	0.937
0.113	0.135	0.128	0.164	0.133	0.150	0.103	0.114	0.930	0.836

Table 4.14: Real time data obtained from n independent sources of User 1 image5 (left iris image)

0.662	0.113	0.973	0.139	0.124	0.113	0.995	0.944	0.095	0.987
0.711	0.113	0.888	0.121	0.138	0.173	0.150	0.850	0.118	0.959
0.867	0.881	0.135	0.117	0.125	0.153	0.969	0.135	0.057	0.595
0.758	0.879	0.915	0.129	0.998	0.115	0.108	0.111	0.993	0.841
0.962	0.128	0.111	0.136	0.149	0.100	0.114	0.121	0.812	0.978
0.834	0.935	0.139	0.948	0.141	0.122	0.125	0.140	0.938	0.122
0.890	0.797	0.949	0.157	0.123	0.906	0.101	0.121	0.086	0.071
0.783	0.121	0.123	0.148	0.158	0.095	0.866	0.128	0.016	0.854
0.843	0.813	0.117	0.133	0.927	0.112	0.096	0.880	0.947	0.736
0.860	0.896	0.122	0.122	0.142	0.123	0.108	0.874	0.114	0.749

Table 4.15: Real time data obtained from n independent sources of User 1 image8 (right iris image)

0.119	0.111	0.998	0.106	0.125	0.126	0.140	0.143	0.102	0.938
0.995	0.125	0.160	0.133	0.129	0.125	0.141	0.123	0.081	0.901
0.976	0.136	0.133	0.968	0.130	0.130	0.140	0.136	0.120	0.805
0.883	0.118	0.149	0.144	0.108	0.112	0.137	0.126	0.867	0.121
0.949	0.111	0.137	0.135	0.154	0.128	0.128	0.101	0.986	0.104
0.906	0.119	0.128	0.139	0.139	0.133	0.136	0.159	0.103	0.136
0.116	0.115	0.128	0.142	0.143	0.132	0.136	0.129	0.993	0.952
0.999	0.143	0.154	0.150	0.141	0.126	0.131	0.135	0.114	0.627
0.129	0.944	0.137	0.133	0.117	0.116	0.122	0.117	0.893	0.053
0.115	0.123	0.111	0.129	0.138	0.126	0.140	0.125	0.979	0.830

Table 4.16: Real time data obtained from n independent sources of User 1 image9 (right iris image)

0.858	0.852	0.989	0.949	0.126	0.142	0.141	0.122	0.883	0.727
0.772	0.119	0.116	0.945	0.977	0.149	0.113	0.113	0.117	0.857
0.660	0.110	0.117	0.130	0.124	0.126	0.140	0.133	0.113	0.713
0.129	0.967	0.958	0.121	0.118	0.125	0.104	0.119	0.119	0.718
0.920	0.884	0.120	0.107	0.148	0.945	0.129	0.098	0.982	0.190
0.113	0.124	0.116	0.122	0.974	0.133	0.115	0.115	0.116	0.926
0.866	0.962	0.127	0.134	0.124	0.152	0.120	0.149	0.089	0.914
0.927	0.912	0.140	0.128	0.119	0.126	0.122	0.097	0.694	0.111
0.849	0.890	0.122	0.113	0.114	0.110	0.114	0.118	0.112	0.827
0.114	0.993	0.120	0.120	0.945	0.127	0.110	0.944	0.844	0.754

Table 4.17: Real time data obtained from n independent sources of User 1 image10 (right iris image)

0.759	0.826	0.797	0.121	0.982	0.132	0.128	0.124	0.157	0.068
0.725	0.969	0.133	0.973	0.127	0.111	0.125	0.110	0.125	0.871
0.111	0.897	0.115	0.146	0.133	0.118	0.125	0.120	0.102	0.857
0.750	0.123	0.120	0.116	0.139	0.114	0.123	0.860	0.119	0.706
0.808	0.118	0.138	0.108	0.130	0.113	0.973	0.128	0.901	0.775
0.896	0.984	0.129	0.128	0.116	0.122	0.115	0.136	0.151	0.692
0.114	0.126	0.115	0.121	0.111	0.118	0.128	0.121	0.937	0.243
0.118	0.125	0.112	0.138	0.130	0.112	0.146	0.109	0.879	0.129
0.972	0.114	0.116	0.109	0.124	0.978	0.119	0.110	0.079	0.769
0.767	0.854	0.117	0.115	0.125	0.127	0.115	0.117	0.921	0.970

4.7.2 Comparison of database and real time data

In matching, we shall compare that how much percent the features of real time data matches with the database. The tables 4.18 to 4.37 shows the percent match of real time data with database.

Table 4.18: Matching percentage of User 1 database and real time images

Database/Real time	User1_image 3	User1_image 4	User1_image 5	User1_image 8	User1_image 9	User1_image 10
User 1_image 1	85	84	84	86	87	88
User 1_image 2	85	85	82	89	87	65
User 1_image 6	90	85	93	86	84	84
User 1_image 7	86	87	80	91	85	93
Max_value	90	87	93	91	87	93

Table 4.19: Matching percentage of User 2 database and real time images

Database/Real time	User2_image 3	User2_imge 4	User2_image 5	User2_image 8	User2_image 9	User2_imge 10
User 2_image 1	64	87	85	89	89	89
User 2_image 2	65	86	90	63	87	86
User 2_image 6	90	89	88	61	85	89
User 2_image 7	88	86	82	92	91	86
Max_value	90	89	90	92	91	89

Table 4.20: Matching percentage of User 3 database and real time images

Database/Real time	User3_image 3	User3_image 4	User3_image 5	User3_image 8	User3_image 9	User3_image 10
User 3_image 1	92	89	91	64	65	85
User 3_image 2	89	86	91	84	89	91
User 3_image 6	85	88	84	84	88	86
User 3_image 7	91	61	91	87	63	86
Max_value	92	89	91	87	89	91

Table 4.21: Matching percentage of User 4 database and real time images

Database/Real time	User4_image 3	User4_image 4	User4_image 5	User4_image 8	User4_image 9	User4_image 10
User 4_image 1	89	89	86	77	84	82

User 4_image 2	84	89	90	77	80	80
User 4_image 6	82	90	82	78	82	88
User 4_image 7	85	87	85	71	80	79
Max_value	89	90	90	78	84	88

Table 4.22: Matching percentage of User 5 database and real time images

Database/Real time	User5_image 3	User5_image 4	User5_image 5	User5_image 8	User5_image 9	User5_image 10
User 5_image 1	85	89	86	84	84	88
User 5_image 2	89	83	92	82	88	89
User 5_image 6	92	90	85	63	92	87
User 5_image 7	84	88	87	86	89	89
Max_value	92	90	92	86	92	89

Table 4.23: Matching percentage of User 6 database and real time images

Database/Real time	User6_image 3	User6_image 4	User6_image 5	User6_image 8	User6_image 9	User6_image 10
User 6_image 1	88	61	87	85	61	84
User 6_image 2	89	88	84	61	93	88
User 6_image 6	90	88	64	89	95	86
User 6_image 7	65	89	89	85	87	87
Max_value	90	89	89	89	95	88

Table 4.24: Matching percentage of User 7 database and real time images

Database/Real time	User7_image 3	User7_image 4	User7_image 5	User7_image 8	User7_image 9	User7_image 10
User 7_image 1	84	89	61	89	63	84
User 7_image 2	89	88	89	63	88	89
User 7_image 6	86	86	91	88	89	93
User 7_image 7	89	85	88	63	89	87
Max_value	89	89	91	89	89	93

Table 4.25: Matching percentage of User 8 database and real time images

Database/Real	User8_image	User8_image	User8_image	User8_image	User8_image	User8_image

time	3	4	5	8	9	10
User 8_image 1	88	89	87	91	89	88
User 8_image 2	86	85	85	84	89	86
User 8_image 6	63	87	93	88	86	63
User 8_image 7	92	88	86	85	85	92
Max_value	92	89	93	91	89	92

Table 4.26: Matching percentage of User 9 database and real time images

Database/Real time	User9_image 3	User9_image 4	User9_image 5	User9_image 8	User9_image 9	User9_image 10
User 9_image 1	90	89	88	88	91	86
User 9_image 2	62	64	85	84	62	89
User 9_image 6	62	89	84	86	63	88
User 9_image 7	89	86	90	92	64	88
Max_value	90	89	90	92	91	89

Table 4.27: Matching percentage of User 10 database and real time images

Database/Real time	User10_img3	User10_img 4	User10_img 5	User10_img8	User10_img9	User10_img10
User 10_img1	63	85	89	87	63	65
User10_img 2	84	87	88	85	87	63
User10_img 6	84	88	90	93	87	89
User10_img 7	87	90	88	85	92	86
Max_value	87	90	90	93	92	89

Table 4.28: Matching percentage of User 11 database and real time images

Database/Real time	User11_img3	User11_img 4	User11_img 5	User11_img8	User11_img9	User11_img10
User 11_img1	89	85	88	91	89	87
User11_img 2	88	92	85	88	89	84
User11_img 6	90	90	89	85	87	92
User11_img 7	86	89	86	86	89	89
Max_value	90	92	89	91	89	92

Table 4.29: Matching percentage of User 12 database and real time images

Database/Real time	User12_img3	User12_img 4	User12_img 5	User12_img8	User12_img9	User12_img10
User 12_img1	90	93	88	89	85	83
User12_img 2	85	89	85	87	90	85
User12_img 6	86	91	91	91	84	86
User12_img 7	93	89	90	93	88	85
Max_value	93	93	91	93	90	86

Table 4.30: Matching percentage of User 13 database and real time images

Database/Real time	User13_img3	User13_img 4	User13_img 5	User13_img8	User13_img9	User13_img10
User13_img1	89	90	86	91	84	88
User13_img 2	86	87	92	87	89	91
User13_img 6	89	93	84	87	86	88
User13_img 7	93	86	93	88	85	84
Max_value	93	93	93	91	89	91

Table 4.31: Matching percentage of User 14 database and real time images

Database/Real time	User14_img3	User14_img 4	User14_img 5	User14_img8	User14_img9	User14_img10
User14_img1	75	83	71	82	81	77
User14_img 2	63	89	72	84	73	86
User14_img 6	70	88	69	86	76	84
User14_img 7	61	91	74	87	82	85
Max_value	75	91	74	87	82	86

Table 4.32: Matching percentage of User 15 database and real time images

Database/Real time	User15_img3	User15_img 4	User15_img 5	User15_img8	User15_img9	User15_img10
User15_img1	81	84	80	83	83	91
User15_img 2	80	77	67	70	71	69
User15_img 6	86	87	84	76	84	85
User15_img 7	72	71	72	72	64	61
Max_value	86	87	84	83	84	91

Table 4.33: Matching percentage of User 16 database and real time images

Database/Real time	User16_img3	User16_img 4	User16_img 5	User16_img8	User16_img9	User16_img10
User16_img1	81	88	92	89	87	88
User16_img 2	89	87	87	89	89	89
User16_img 6	90	84	89	85	84	88
User16_img 7	85	90	89	84	84	84
Max_value	90	90	92	89	89	89

Table 4.34: Matching percentage of User 17 database and real time images

Database/Real time	User17_img3	User17_img 4	User17_img 5	User17_img8	User17_img9	User17_img10
User17_img1	90	89	87	87	91	87
User17_img 2	87	63	86	86	86	92
User17_img 6	86	89	86	87	90	86
User17_img 7	64	94	64	89	93	89
Max_value	90	94	87	89	93	92

Table 4.35 Matching percentage of User 18 database and real time images

Database/Real time	User18_img3	User18_img 4	User18_img 5	User18_img8	User18_img9	User18_img10
User18_img1	60	60	56	52	60	54
User18_img 2	64	64	56	60	52	64
User18_img 6	52	71	56	71	61	64
User18_img 7	64	67	64	64	52	64
Max_value	64	71	64	71	60	64

Table 4.36: Matching percentage of User 19 database and real time images

Database/Real time	User19_img3	User19_img 4	User19_img 5	User19_img8	User19_img9	User19_img10
User19_img1	93	86	88	91	89	86
User19_img 2	88	88	89	88	85	88
User19_img 6	63	87	89	86	89	62
User19_img 7	86	85	89	88	93	87
Max_value	93	88	89	91	93	88

Table 4.37: Matching percentage of User 20 database and real time images

Database/Real time	User20_img3	User20_img 4	User20_img 5	User20_img8	User20_img9	User20_img10
User20_img1	87	86	89	87	87	86
User20_img 2	92	90	88	93	87	87
User20_img 6	87	85	85	93	89	63
User20_img 7	87	87	89	87	88	86
Max_value	92	90	89	93	89	87

Now, we shall collect the matching features according to different ranges of various users as shown in table 4.38.

Table 4.38: Matching percentage for individual users

Users	Matching percentage for individual users (4x6 each)			
	>= 90%	>80 & <90%	>70 & <80%	>60 & <70%
User 1	4	2	0	0
User 2	4	2	0	0
User 3	3	3	0	0
User 4	2	3	1	0
User 5	4	2	0	0
User 6	2	4	0	0
User 7	2	4	0	0
User 8	4	2	0	0
User 9	4	2	0	0
User 10	4	2	0	0
User 11	4	2	0	0
User 12	5	1	0	0

User 13	5	1	0	0
User 14	1	3	2	0
User 15	1	5	0	0
User 16	3	3	0	0
User 17	4	2	0	0
User 18	0	0	2	4
User 19	3	3	0	0
User 20	3	3	0	0
Total images→ 20*6	62	49	5	4

In order to calculate the percentage of false matching among 20 user we have calculate the following result which are shown in Table 4.39.

Table 4.39 Matching percentage of different users among each other

USERS	1	2	3	4	5	6	7	8	9	10	11	12	13	14	15	16	17	18	19	20
1	100	8	9	7	17	10	10	7	6	9	12	15	10	3	14	9	11	12	16	13
2	9	100	11	5	14	15	9	11	8	10	8	15	11	5	11	5	12	10	6	9
3	8	9	100	10	12	10	10	8	7	11	10	13	12	4	9	12	6	8	13	10
4	7	5	10	100	12	6	13	9	12	12	5	10	6	9	12	10	10	14	11	9
5	15	15	10	12	100	8	17	13	8	11	10	10	10	6	12	4	7	10	12	11
6	11	14	10	6	11	100	12	9	12	12	14	16	8	6	9	9	16	11	9	12
7	10	9	8	10	14	12	100	15	13	17	18	9	13	6	10	4	11	16	4	11
8	7	11	7	9	11	10	12	100	9	13	6	5	7	3	17	2	10	17	9	9
9	7	8	7	12	9	11	11	11	100	19	11	13	10	4	6	8	18	14	14	10
10	8	11	9	11	11	13	19	19	18	100	14	13	10	11	14	7	10	12	10	11
11	10	9	10	5	11	13	16	6	12	13	100	10	7	5	12	6	9	13	10	11
12	16	14	13	10	11	16	9	5	12	13	11	100	11	6	8	7	15	13	9	12
13	10	10	13	5	9	7	13	7	9	10	8	12	100	6	14	6	11	10	12	12
14	3	4	3	8	6	6	5	3	4	10	4	7	7	100	6	5	4	8	8	3

15	13	13	8	12	15	9	12	15	5	13	11	7	12	7	100	8	11	11	8	9
16	9	5	12	10	5	8	4	2	7	10	8	8	7	5	8	100	4	7	12	9
17	11	12	6	10	8	16	11	10	17	10	8	16	12	5	10	4	100	15	14	11
18	12	11	8	13	11	12	19	17	14	12	13	13	10	7	12	7	12	100	16	8
19	15	6	16	8	9	8	4	8	11	10	10	11	11	6	7	11	14	15	100	5
20	13	9	9	8	11	11	14	10	11	12	12	14	12	3	11	8	12	7	6	100

In order to check the similarity features or similar independent source available in different users we have performed the cross matching operation and have obtained the table 4.39. It is clear from the table that when we match the templates of the same user it gives a matching rate of 100% which is obvious. Furthermore, the matching percentage among different user is also shown in the table 4.39. In case of different users matching, none of the matching percentage of independent sources are exceeding to 20%, which makes this method a very useful approach to identify the imposter out of a large database.

Conclusion

A blind source separation technique i.e. ICA has been presented and is used to eliminate the problem of iris recognition. ICA is a new concept in the field of image processing which helps in determining a number of sources or features (independent components) from segmented image. It is conclude that the proposed method is very predicting and can help in improving the identification rate of iris systems. Here, iris localization or segmentation helped in determining the iris boundary in order not to include the other part of the eye and eyelashes. Iris localization also helped to make the algorithm immune to noise and garbage data.

Iris recognition experiment has been tested on 200 images of the CASIA standard database for the iris images. The framework developed here is divided in various segments like segmentation, centering, whitening and normalization. These preprocessing steps are used to make sure the proper fetching of the independent components from the iris image. Blind source separation accuracy was evaluated over 10 images of each user of 100x100 pixels size each. When the procedure is followed in a significant manner, a database is created for first four images of each user and other 6 images as the real time data which are used to check the percentage matching with database. In a very specific manner we have examined that for the first user we have got a matching percentage of 90% or above around 4 times and it is in between 80-90% around 19 times out of 24 matching (4x6, 4images for data base and 6 Images for real time run). Similarly, we have calculated the matching percentage for other 19 users and have got significant results. ICA is specifically more robust and effective in signal source separation in signal processing, but we have shown a good performance over iris images too.

Future works

As we have already discussed that ICA algorithm is mainly used for the signal processing, but we have explored it for the image processing. Thus, this field of image processing can be enhanced using various methods of independent component analysis. In my dissertation, I had used the kurtosis method of ICA which is a curve based technique; we can also make use of the entropy based Negentropy method for the feature extraction in an image.

In the result section we have noticed that our matching percentage is mainly between 80 to 90%, so in order to get a higher matching percent, a proper localization technique needs to be developed.

References:

[1] Jain, A. K., Ross, A. and Prabhakar, S. “An Introduction to Biometric Recognition”, IEEE transactions on circuits and systems for video technology, vol. 14, no. 1, pp. 4–20., Jan 2004.

[2] Matsumoto, T., Hoshino, H., Yamada, K. and Hasino, S. “Impact of artificial gummy fingers on fingerprint systems”, In Proc. of SPIE, Volume 4677, Feb. 2002, pp. 275–289.

[3] Hong, L. and Jain, A. K. “Integrating faces and fingerprints for personal identification” IEEE Trans. Pattern Anal. Mach. Intell., Volume 20, No. 12, Dec. 1998, pp. 1295–1307.

[4] Ross, A. and Govindarajan, R. “Feature level fusion using hand and face Biometric”, In Proc. of SPIE Conf. Biometric Technology for Human Identification II, Mar. 2005, pp. 196–204.

[5] Jain, A. K., Ross, A. and Pankanti, S. "Biometric: A Tool for Information Security", IEEE Transactions on Information Forensics And Security, Volume 1, issue 2, Jun. 2006, pp 125 – 144.

[6] Cappelli, R., Maio, D., Maltoni, D., Wayman, J. L. and Jain, A.K. “Performance evaluation of fingerprint verification systems”, IEEE Trans. Pattern Anal. Mach. Intell., Volume 28, issue 1, Jan. 2006, pp. 3–18.

[7] Jain, A. K., Hong, L. and Bolle, R. “On-line fingerprint verification”, IEEE Transactions on Pattern Recognition and Machine Intelligence, Volume 19, No. 4, Aug. 1996, pp. 302–314.

[8] Hong, L. and Jain, A. K. “Integrating faces and fingerprints for personal identification” IEEE Trans. Pattern Anal. Mach. Intell., Volume 20, No. 12, Dec. 1998, pp. 1295–1307.

[9] Bhattacharyya, D., Ranjan, R., Alisherov, A.F. and Choi, M. “Biometric Authentication: A Review", International Journal of u- and e- Service, Science and Technology, Vol. 2, No. 3, September, 2009

[10] Dabbah, M. A., Woo, W. L. and Dlay, S. S. "Secure Authentication for Face Recognition," In Proc. of IEEE Symposium on Computational Intelligence in Image and Signal Processing, Apr. 2007. USA, pp. 121 - 126.

[11] Hong, L. and Jain, A. K. “Integrating faces and fingerprints for personal identification”, IEEE Trans. Pattern Anal. Mach. Intell., Volume 20, No. 12, Dec. 1998, pp. 1295–1307.

[12] Ross, A. and Govindarajan, R. “Feature level fusion using hand and face Biometric”, In Proc. of SPIE Conf. Biometric Technology for Human Identification II, Mar. 2005, pp. 196–204.

[13] Li, S. Z. and Jain, A. K. Eds., Handbook of Face Recognition. New York: Springer Verlag, 2004.

[14] Cardinaux, F., Sanderson, C. and Bengio, S. “User Authentication via Adapted Statistical Models of FaceImages”, IEEE Transaction on Signal Processing, Volume 54, Issue 1, Jan. 2006, pp. 361 - 373.

[15] Mason, J. S. and Brand, J. D. "The Role of Dynamics in Visual Speech Biometric", proceedings of IEEE International Conference on Acoustics, Speech and Signal Processing, Orlando, Florida, pp.142-147, 2002

[16] Thomas RUGGLES, “Comparison of biometric techniques”.

[17] Ganorkar, S. R., and Ghatol, A. A. “Iris Recognition: An Emerging Biometric Technology”, In Proc. of the 6th WSEAS International Conference on Signal Processing, Robotics and Automation, Greece, Feb. 2007, pp. 91 – 96.

[18] Daugman, J. “The importance of being random: statistical principles of iris recognition”, Journal of Pattern Recognition, Elsevier, Volume 36, No. 2, Feb. 2003, pp. 279–291.

[19] Bandopadhaya, S.K., Bhattacharyya, D., Mukherjee, S., Ganguly, D. and Das, P.“Statistical Approach for Offline Handwritten Signature Verification”, Journal of Computer Science, Science Publication, Volume 4, Issues 3, May. 2008, pp. 181 – 185.

[20] Wayman, J. L. “Fundamentals of Biometric Authentication Technologies”, International Journal of Image and Graphics, World Scientific Publication, Volume 1, No. 1, Jan. 2001, pp. 93-113.

[21] Furui, S. "Recent Advances in Speaker Recognition", In Proc. of First International Conference on Audio and Video based Biometric Person Authentication, UK, Mar. 1997, pp. 859-872.

[22] Reid, P. "Biometric for Network Security", First Indian reprint, Pearson Education, 2004.

[23] Soutar, C. "Implementation of Biometric System-Security and Privacy Considerations", Information security Technical report, vol.7, no.4, Dec 2002.

[24] Jain, A. K., Ross A. and Pankanti, S. “A proto- type Hand Geometry- based Verification System", 2nd International Conference on Audio and Video based Biometric Personal Authentication, Washington, USA, PP. 166-171, 199.

[26] Cannon, M., Byrne, M., Cotter, D., Sham, P., Larkin, C. and O'Callaghan, E. "Further Evidence for Anomalies in the hand-prints of patients and Schizophrenia: A study of Secondary Creases", Schizophrenia Research, vol.13,pp. 179-184, 1994.

[27] Kong, A., Zhang, D. and Lu, G. "A study of Identical twins palm print for Personal Verification", Pattern Recognition, vol.39, no.11, pp. 2149-2156, 2006.

[28] Hocquet, S., Ramel, J. and Cardot, H. “Fusion of Methods for Keystroke Dynamic Authentication”, In Proc. of 4th IEEE Workshop on Automatic Identification Advanced Technologies, USA, Oct. 2005, pp. 224 – 229.

[29] Monrose, F. and Rubin, A. “Authentication via keystroke dynamics”, In Proc. of 4th ACM Conference on Computer and Communications Security, Switzerland, Apr. 1997, pp. 48–56.

[30] Im, S., Park, H., Kim, Y., Han, S., Kim, S., Kang, C. and Chung, C. “A Biometric Identification System by Extracting Hand Vein Patterns”, Journal of the Korean Physical Society, Korean Publication, Volume 38, Issue 3, Mar. 2001, pp. 268-272.

[31] Jain, A. K., Pankanti, S., Prabhakar, S., Hong, L., Ross, A. and Wayman, J. L. "Biometric: a grand challenge", In Proc. of International Conference on Pattern Recognition, Cambridge, U.K., Aug. 2004, pp. 935 - 942.

[32] Phillips, J., Martin, A., Wilson, C. and Przybocki, M. "An introduction to evaluating biometric systems", IEEE Computer Society., Volume 33, No. 2, Feb. 2000, pp. 56–63.

[33] Wayman, J. L., Jain, A. K., Maltoni, D. and Maio, D. Eds., "Biometric Systems: Technology, Design and Performance Evaluation", New York: Springer Verlag, 2005.

[34] Vision Aware website < http://www.visionaware.org/aging-eye-low-vision>

[35] Daugman, J. 2004 (How iris works)

[36] Daugman, J. and Downing, C.. Epigenetic randomness, complexity and singularity of human iris patterns. Proceedings of the Royal Society of London- B, 268:1737–1740, 2001.

[37] Bertillon, A. La couleur de l'iris. Revue scientifique, 36(3):65–73, 1885.

[38] Hazem, M. El-Bakry. Fast iris detection for personal identification using modular neural networks. In IEEE Int. Symp. on Circuits and Systems, pages 52–55, 2001.

[39] Johnston, R. Can iris patterns be used to identify people? Los Alamos National Laboratory, Chemical and Laser Sciences Division Annual Report LA-12331-PR, June 1992. Pages 81-86.

[40] Daugman, J. Biometric personal identification system based on iris analysis. U.S. Patent No.5,291,560, March 1994.

[41] Daugman, J. High confidence visual recognition of persons by a test of statistical independence. IEEE Transactions on Pattern Analysis and Machine Intelligence, 15(11):1148–1161, November 1993.

[42] Daugman, J. New methods in iris recognition. IEEE Transactions on Systems, Man and Cybernetics - B, to appear.

[43] Wyatt, H.. A minimum wear-and-tear meshwork for the iris. Vision Research, 40:2167–2176, 2000.

[44] Wildes, R. P. Iris recognition: An emerging biometric technology. Proceedings of the IEEE, 85(9):1348–1363, September 1997.

[45] Wildes, R. P. Automated, non-invasive iris recognition system and method. U.S. Patent No. 5,572,596 and 5,751,836, 1996 and 1998.

[46] Wildes, R. P. Iris recognition: An emerging biometric technology. Proceedings of the IEEE, 85(9):1348–1363, September 1997.

[47] Wildes, R. P. Iris recognition. In Biometric Systems: Technology, Design and Performance Evaluation, pages 63–95. Spring-Verlag, 2005.

[48] Nanavati, S., Thieme, M. and Nanavati, R. 2002. Biometrics: identity verification in a networked world, John Wiley & Sons, New York, U.S.A., pp 1-300.

[49] Rhodes, K.A. 2002. National Preparedness: Technologies to Secure Federal Buildings. United States General Accounting Office (GAO), April 25, 2002 1-72.

[50] CY Lab (2011). Iris and face recognition.

http://www.cylab.cmu.edu/partners/success-stories/iris-recognition.html [October 5, 2011]

[51] Hanna, K., Mandelbaum, R., Mishra, D., Paragano, V. and Wixson, L. 1996. A system for non-intrusive human iris acquisition and identification. Proceedings of the International Association of Pattern Recognition Workshop on Machine Vision Applications, Tokyo, Japan, November 12-14, 1996, 200-203.

[52] Park, K.R. and Kim, J. 2005. A real-time focusing algorithm for iris recognition camera. Institute of the Electrical and Electronic Engineers Transactions on Systems, Man, and Cybernetics, 35, 441-444.

[53] Fancourt, C., Bogoni, L., Hanna, K., Guo, Y., Wildes, R., Takahashi, N. and Jain, U. 2005. Iris recognition at a distance. Proceedings of the International Conference on Audio-

and Video-Based Biometric Person Authentication. Hilton Rye Town, New York, U.S.A., July 20-22, 2005, 1–13.

[54] He, Y., Cui, J., Tan, T. and Wang, Y. 2006. Key techniques and methods for imaging iris in focus. Proceedings of the 18th International Conference on Pattern Recognition, Hong Kong, September 18, 2006, 557–561.

[55] Eyetrackingupdate (2010). Beware of problems with iris recognition.

http://eyetrackingupdate.com/2010/11/03/beware-problems-iris-recognition/ [November 7, 2011]

[56] Ma, L., Tan, T., Wang, Y. and Zhang, D. 2003. Personal identification based on iris texture analysis. Institute of Electrical and Electronic Engineers Transactions on Pattern Analysis and Machine Intelligence. 25, 1519-1533.

[57] Wei, Z., Tan, T., Sun, Z. and Cui, J. 2006. Robust and fast assessment of iris image quality. Proceedings of the International Conference on Advances in Biometrics, Hong Kong, China, January 5-7, 2006, 464-470.

[58] Bachoo, A.K. and Tapamo, J.R. 2005. Texture detection for segmentation of iris images. Proceedings of the Annual Research Conference of the South African Institute of Computer Information Technologists, South Africa, September 20-22, 2005, 236–243.

[60] Daugman, J. 1993. High confidence visual recognition of persons by a test of statistical independence. Institute of Electrical and Electronic Engineers Transactions on Pattern Analysis Machine Intelligence. 15, 1148–1161.

[61] Daugman, J. 2003. The importance of being random: Statistical principles of iris recognition. Pattern Recognition. 36, 279-291.

[62] Avila, S.C. and Reillo, S.R. 2005. Two different approaches for iris recognition using Gabor filters and multiscale zero-crossing representation. Pattern Recognition. 38, 231–240.

[63] Jain, A.K., Ross, A. and Prabhakar, S. 2004. An introduction to biometric recognition. Institute of Electrical and Electronic Engineers Transactions on Circuits and Systems for Video Technology. 14, 4-20.

[64] Matey, J.R., Naroditsky, O., Hanna, K., Kolcyznski, R., LoIacono, D.J., Mangru, S., Tinker, M., Zappia, T.M. and Zhao, W.Y. 2006. Iris on the move: Acquisition of images for iris recognition in less constrained environments. Proceedings of the Institute of Electrical and Electronic Engineers. Princeton, U.S.A., November 11, 2006, 1936-1947.

[65] Daugman, J. 2007. New methods in iris recognition. Institute of Electrical and Electronic Engineers Transactions on Systems, Man, and Cybernetics. 37, 1167 – 1175.

[66] Lorenz, M.G., Mengibar, L., Liu, J. and Fernandez, B. 2008. User-friendly biometric camera for speeding iris recognition systems. Proceedings of the 42nd Annual Institute of Electrical and Electronic Engineers International Carnahan Conference on Security Technology, Prague, October 13-16, 2008, 241 – 246.

[67] Pan, L. and Xie, M. 2005. Research on iris image preprocessing algorithm. Proceedings of the Institute of Electrical and Electronic Engineers International Symposium on Communications and Information Technology, Chengdu, China, October 12-14, 2005, 161-164.

[68] Chowhan, S.S. and Shinde, G.N. 2009. Evaluation of statistical feature encoding techniques on iris images. Proceedings of the World Research Institutes World Congress on Computer Science and Information Engineering. Los Angeles, CA, March 31- April 2, 2009, 71-75.

[69] Gupta, P., Mehrotra, H., Rattani, A., Chatterjee, A. and Kaushik, A.K. 2006. Iris recognition using corner detection. Proceedings of the 23rd International Biometric Conference, Montreal, Canada, July 16-21, 2006, 1-5.

[70] Gonzaga, A. and Dacosta, R.M. 2009. Extraction and selection of dynamic features of the human iris. Proceedings of the XXII Brazilian Symposium on Computer Graphics and Image Processing. Sarajevo, Brazil, October 11-15, 2009, 202-208.

[71] Sky imaging (2011). *Automatic preprocessing* of planetary *images* with Iris.

http://www.skyimaging.com/registration-auto-lrgb.php [October 15, 2011]

[72] Lei, X. and Fei, S. P. 2003. A quality evaluation method of iris images. Chinese Journal of Stereology and Image Analysis, 7, 108-112.

[73] Kalka, N.D., Zuo, J., Schmid, N.A. and Cukic, B. 2006. Image Quality assessment for Iris Biometric. Proceedings of the Society of Photo Optical Instrumentation Engineers, Orlando, FL, U.S.A., April 17, 2006, 1-2.

[74] Ma, L., Wang, Y. and Tan, T. 2002. Iris recognition based on multichannel gabor filtering. Proceedings of the 5th Asian Conference on Computer Vision. Melbourne, Australia, January 23-25, 2002, 1-5.

[75] Moorthi, M., Arthanari, M. and Sivakumar, M. 2010. Preprocessing of video image with unconstrained background for drowsy driver detection. International Journal of Computer Science and Information Security, 8, 145-151.

[76] Proenca, H. and Alexandre, L.A. 2006. Iris segmentation methodology for non-cooperative recognition. Proceedings of the Institute of Electrical and Electronic Engineers on Vision, Image and Signal Processing, Coviha, Portugal, April 6, 2006, 199–205.

[77] Tuceryan, M. 1994. Moment based texture segmentation. Pattern Recognition Letters, 15, 659–668.

[78] Wildes, R.P. 1997. Iris recognition: An emerging biometric technology. Institute of the Electrical and Electronic Engineers Special Issue on Automated Biometrics, 85, 1348–1363.

[79] Camus, T.A. and Wildes, R.P. 2002. Reliable and fast eye finding in close-up images. Proceedings of the International Conference on Pattern Recognition, Quebec, Canada, August 11-15, 2002, 389–394.

[80] Noh, S., Bae, K., Park, K. R. and Kim, J. 2005. A new iris recognition method using independent component analysis. Institute of Electronics, Information and Communication Engineers Transactions on Information and Systems, E88-D, 2573-2581.

[81] Ma, L., Tan, T., Wang Y. and Zhang, D. 2004. Efficient iris recognition by characterizing key local variations. Institute of Electrical and Electronic Engineers Transactions on Image Processing. 13, 739–750.

[82] Miyazawa, K., Ito, K., Aoki, T., Kobayashi, K. and Nakajima, H. 2005. An efficient iris recognition algorithm using phase-based image matching. Proceedings of the Institute of Electrical and Electronic Engineers International Conference on Image Processing. Sendai, Japan, September 11-14, 2005, 49-52.

[83] Adelson, E.H., Anderson, C.H., Bergen, J.R., Burt, P.J. and Ogden, J.M. 1984. Pyramid methods in image processing. Radio Corporation of America Engineer. 29, 33-41.

[84] Cole, L., Austin, D. and Cole, L. 2004. Visual object recognition using template matching. Proceedings of the Australian Conference on Robotics and Automation. Canberra, Australia, December 6 - 8, 2004, 1-8.

[85] Khaw, P., 2002. Iris Recognition Technology for Improved Authentication. Sysadmin Audit Networking and Security, Security Essentials Practical Assignment, 1.3, 1-14.

[86] Hotelling, H. (1933), ‘Analysis of a complex of statistical variables into principal components’, Journal of Educational Psychology 24, 417–441, 498–520.

[87] Rodriguez, J.J. Rotation Forest: A New Classifier Ensemble Method, IEEE Transactions on Pattern Analysis and Machine Intelligence. Oct. 2006, vol.28, 1619 – 1630

[88] http://en.wikipedia.org/wiki/Linear_discriminant_analysis

[89] M. Bartlett and T. Sejnowski. Independent components of face images: A representation for face recognition. In Proc. the 4th Annual Joint Symposium on Neural Computation, Pasadena, CA, May 17, 1997.

[90] Aapo Hyvärinen and Erkki Oja. Independent Component Analysis: Algorithms and Applications. Neural Networks, 13(4-5):411-430, 2000

[91] Ganesh R. Naik and Dinesh K Kumar. An Overview of Independent Component Analysis and Its Applications. Informatica 35 (2011) 63–81

[92] Jan Eriksson. Contributions to Theory and Algorithms of Independent Component Analysis and Signal Separation. Dissertation for the degree of Doctor of Science in Technology to be presented with due permission of the Department of Electrical and Communications Engineering for public examination and debate in Auditorium S4 at Helsinki University of Technology (Espoo, Finland) on the 20th of August, 2004

[93] Behera S. K 2009. Fast ICA for Blind Source Separation and Its Implementation

[94] Mingxing He, Shi-Jinn Horng, Pingzhi Fan, Ray-Shine Run, Rong-Jian Chen, Jui-Lin Lai, Muhammad Khurram Khan, Kevin Octavius Sentosa. Performance evaluation of score level fusion in multimodal biometric systems

[95] F.R. Hampel, P.J. Rousseeuw, E.M. Ronchetti, W.A. Stahel, Robust Statistics: The Approach Based on Influence Functions, Wiley, 1986.

[96] J.E. Jackson. A User's Guide to Principal Components. New York: John Wiley and Sons, 1991.

[97] Jollife, I.T. Principal Component Analysis. Springer-Verlag, 1986.

[98] Vempala, S. S. The Random Projection Method, volume 65. American mathematical Society, 2004.

[99] Kaski, S. Dimensionality reduction by random mapping: fast similarity computation for clustering. In Proceedings of International Joint Conference on Neural Networks, pages 413–418, 1998

[100] Bingham, E. and Mannila, H. Random projection in dimensionality reduction: applications to image and text data. In KDD ’01: Proceedings of the seventh ACM SIGKDD international conference on Knowledge discovery and data mining, pages 245–250, New York, NY, USA, 2001. ACM.

[101] Goel, N., Bebis, G. and Nefian, A. Face recognition experiments with random projection. volume 5779, pages 426–437. SPIE, 2005

[102] Magen, A. Dimensionality reductions that preserve volumes and distance to ane spaces, 2002.

[103] Dasgupta, S. Experiments with random projection. In UAI ’00: Proceedings of the 16th Conference on Uncertainty in Artificial Intelligence, pages 143–151, San Francisco, CA, USA, 2000. Morgan Kaufmann Publishers Inc.

[104] Hyvärinen, A. (1999a). Fast and robust fixed-point algorithms for independent component analysis. IEEE Transactions on Neural Networks, 10(3):626–634.

[105] Giannakopoulos, X., Karhunen, J., and Oja, E. (1998). Experimental comparison of neural ICA algorithms. In Proc. Int. Conf. on Artificial Neural Networks (ICANN’98), pages 651–656, Skövde, Sweden.

[106] benlin, X., Fangfang, Li., xingliang, M. and Huazhong, J. Study on Independent Component Analysis’ Application in Classification and change Detection of Multispectral Images. The International Archives of the Photogrammetry, Remote Sensing and Spatial Information Sciences. Vol. XXXVII. Part B7. Beijing 2008

[107] Papoulis, A. (1991). Probability, Random Variables, and Stochastic Processes. McGraw-Hill, 3rd edition.

[108] Cover, T. M. and Thomas, J. A. (1991). Elements of Information Theory. Wiley.

[109] Patrik O. Hoyer1 and Aapo Hyvärinen. Independent Component Analysis Applied to Feature Extraction from Colour and Stereo Images. *Network: Computation in Neural Systems* 11: 191-210 [August, 2000]

[110] http://www.cbsr.ia.ac.cn/IrisDatabase.htm